

Original Research

EZH2i EPZ-6438 and HDACi vorinostat synergize with ONC201/TIC10 to activate integrated stress response, DR5, reduce H3K27 methylation, ClpX and promote apoptosis of multiple tumor types including DIPG ☆,☆☆,★**Yiqun Zhang**^{a,b,c,d}; **Lanlan Zhou**^{a,b,c,d};
Howard Safran^{b,d,e}; **Robyn Borsuk**^{a,f}; **Rishi Lulla**^{b,d,f};
Nikos Tapinos^{b,d,g}; **Attila A. Seyhan**^{a,b,c,d};
Wafik S. El-Deiry^{a,b,c,d,g,h}^a Laboratory of Translational Oncology and Experimental Cancer Therapeutics, The Warren Alpert Medical School, Brown University, Providence, RI, USA^b The Joint Program in Cancer Biology, Brown University and Lifespan Health System, Providence, RI, USA^c Department of Pathology and Laboratory Medicine, The Warren Alpert Medical School, Brown University, Providence, RI, USA^d Cancer Center at Brown University, The Warren Alpert Medical School, Brown University, Providence, RI, USA^e Hematology/Oncology Division, Department of Medicine, Lifespan Health System and Brown University, Providence, RI, USA^f Pediatric Hematology/Oncology, The Warren Alpert Medical School, Brown University, Providence, RI, USA^g Department of Neurosurgery, The Warren Alpert Medical School, Brown University, Providence, RI, USA**Abstract**

ONC201/TIC10 activates TRAIL signaling through ATF4 and the integrated stress response (ISR). ONC201 demonstrated tumor regressions and disease stability in patients with histone H3K27M-mutated midline-glioma. H3K27M-mutation prevents H3K27-methylation on the mutated allele. EZH2 inhibitors (EZH2i) reduce H3K27 methylation and have anti-tumor effects. We hypothesized ONC201 sensitivity and tumor apoptosis may increase by reducing H3K27-methylation with EZH2i or HDACi as mimics of H3K27M-mutation. EZH2i EPZ-6438 (tazemetostat) or PF-06821497 and HDACi vorinostat were combined with ONC201 to treat multiple cancer cell lines and cell viability and histone modifications were analyzed. We observed synergistic effects towards cell viability in multiple cancers by EPZ-6438 or PF-06821497 plus ONC201 or triple therapy with vorinostat, EPZ-6438, and ONC201. EPZ-6438 and vorinostat synergized with ONC201 to enhance apoptosis. Activation of the ISR and TRAIL-DR5 were observed in cells treated with ONC201 +/- epigenetic modulators. Knockdown of ATF4 reduced DR5 induction and apoptosis following EZH2i and ONC201 treatment of U251 glioma cells. mRNA expression of dopamine-receptors did not correlate with ONC201 sensitivity in the tumor cell lines tested (N = 12), including changes after epigenetic drugs. Dopamine did not rescue apoptosis by ONC201 in different tumor cell lines (N = 10) including 2 GBM, 3 DIPG and did not prevent DR5 activation or apoptosis. DRD2 agonist sumanilole did not protect brain tumor cells (N = 6 including 4 DIPG cell lines) from ONC201 reduction in viability. Although synergy was observed with ONC201 and vorinostat, there was no significant increase in H3K27 acetylation in cell lines including DIPG as compared to vorinostat alone, and in some cases the acetylation was less than vorinostat alone at 72 H.

* Corresponding author

E-mail address: wafik@brown.edu (W.S. El-Deiry).

☆ This work was presented in part at the 2020 American Association for Cancer Research meeting.

☆☆ Funding: W.S.E-D. is an American Cancer Society Research Professor and is supported by the Menco Family University Professorship at Brown University. This work was supported by an NIH grant (CA173453) to W.S.E-D.

*☆☆ Conflicts of interest: W.S.E-D. is a co-founder of Oncoceutics, Inc., a subsidiary of Chimerix. Dr. El-Deiry has disclosed his relationship with Oncoceutics and potential conflict of interest to his academic institution/employer and is fully compliant with the institutional policy that is managing this potential conflict of interest.

Received 5 September 2020; received in revised form 8 June 2021; accepted 9 June 2021

H3K27 methylation reduction correlated with synergy from combinations of either EPZ-6438 or vorinostat with ONC201 or triple combination. Our findings provide a rationale for combination of ONC201 and epigenetic modulators including triple therapy for *in vivo* and clinical testing in treatment of human malignancies including brain tumors and DIPG.

Neoplasia (2021) 23, 792–810

Key Words: ONC201, EZH2, HDAC, Glioma, Breast cancer, Histone methylation, Histone acetylation

Introduction

ONC201/TIC10 (TRAIL-inducing compound #10), the founding member of the imipridone class of small molecules, kills solid tumor cells by triggering an integrated stress response (ISR) dependent on ATF4 activation [1] and presents anti-proliferative and pro-apoptotic effects against a broad range of tumors [2–5]. The mechanism of action of ONC201 involves the engagement of PERK-independent activation of the integrated stress response, leading to tumor upregulation of TRAIL receptor DR5 and dual Akt/ERK inactivation, and consequent Foxo3a activation leading to up-regulation of the death ligand TRAIL [6, 7].

Early clinical data have indicated that ONC201 provides clinical benefit in a subset of brain tumor patients with histone H3K27M-mutated diffuse midline glioma (DMG) [8, 9]. DMG with H3K27M mutation presents a globally reduced H3K27 di- and tri-methylation phenotype and in turn, alters the expression of genes by epigenetic modulation [10]. PRC2 is a multiprotein enzyme complex (EZH2, SUZ12, EED, and YY1) responsible for the methylation of lysine 27 on histone H3 (H3K27me3) [11]. The Enhancer of Zeste Homolog 2 (EZH2) is a histone methyltransferase that tri-methylates H3K27 (H3K27me3) and silences target genes. EZH2 is the functional enzymatic component of the PRC2 that methylates histone H3 at Lysine 27 (H3K27) and silences target genes involved in various functions such as cell cycle, cell proliferation, and cell differentiation [12]. EZH2 inhibitors (EZH2i) reduce global histone H3K27 methylation, leading to the de-repression of target gene transcription and anti-cancer effects [13]. Anti-cancer effects with EZH2i in tumors have been observed in glioma [14, 15], breast cancer [16], lymphoma [17], and multiple myeloma [18]. In 2020, EZH2i EPZ-6438 (tazemetostat) was approved by the FDA for the treatment of relapsed/refractory follicular lymphoma and metastatic or locally advanced epithelioid sarcoma. PF-06821497 is another EZH2i being tested in clinical trials of small cell lung cancer, follicular lymphoma, castration-resistant prostate cancer, and diffuse large B cell lymphoma. [19]

We hypothesized that EZH2i may sensitize tumor cells to ONC201 due to the reduction of global histone H3K27 methylation, in a manner that may mimic H3K27M-mutation that has been associated with ONC201-responsiveness in patients with mid-line glioma. HDACs remove the acetyl groups on the histone and thereby down-regulate the transcription of the target genes including oncogenes and tumor suppressor genes [20]. Histone deacetylase inhibitors (HDACi's) increase levels of histone acetylation leading to a more relaxed chromatin structure and ultimately gene transcription, including those involved in tumor suppression, cell-cycle arrest, cell differentiation, and apoptosis [21]. We hypothesized that epigenetic modulation may sensitize tumor cells to ONC201 and evaluated the synergy of combinations of ONC201 and EZH2i and/or HDACi.

Binding and reporter assays have shown that ONC201 is a selective antagonist of the dopamine D2-like receptors, specifically, DRD2 and DRD3 [22]. Dopamine receptors belong to the superfamily of G-protein-coupled-receptors (GPCRs). Dopamine receptors are classified into two groups, the

D1-like group, and the D2-like group. Dopamine receptor D1 (DRD1) and DRD5 belong to the D1-like group. Stimulation of D1-like receptors increases cyclic AMP levels. DRD2 and DRD3 belong to the D2-like group and their stimulation decreases cyclic AMP levels. DRD5 opposes DRD2 signaling and a DRD2+DRD5- biomarker signature is associated with enhanced ONC201 tumor cell sensitivity [23]. We have also shown that a DRD5 antagonist sensitizes tumor cells to ONC201 [24]. We hypothesized that the interaction between ONC201 and DRD2/DRD3 plays a role in the anti-cancer effects of ONC201 and that dopamine receptor expression may correlate with ONC201 sensitivity. In our study, we investigated the relationship between the expression of dopamine receptors and ONC201 sensitivity spanning different cancer types, the modulation of dopamine receptor expression with epigenetic drugs, and the effects of dopamine or DRD2-agonist sumanirole on ONC201-mediated cell death to determine whether modulation of dopamine receptors is associated with sensitization to ONC201. Our results provide novel insights into the underlying anti-tumor mechanisms of ONC201 against brain tumors with H3K27M mutation, and provide evidence for synergies of ONC201 with epigenetic drugs that may in the future be tested in multiple tumor types including brain tumors or DIPG.

Methods

Cell culture and reagents

The human breast cancer, GBM, gastric cancer, multiple myeloma cell lines were purchased from the American Type Culture Collection (ATCC). All cell lines were confirmed to be mycoplasma free using PCR testing methods. All cell lines were cultured in their ATCC-recommended media supplemented with 10% (v/v) fetal bovine serum and 1% Penicillin/Streptomycin with or without chemotherapy agents at 37°C within a 95% humidified atmosphere containing 5% carbon dioxide in an incubator. Saos2 cells were cultured in medium supplemented with 15% FBS. Human H3K27-M mutated DIPG cell lines were from patients with pediatric gliomas and are described in more detail elsewhere (Borsuk, R., Zhou, L., Chang, W-I, Zhang, Y., Sharma, A., Prabhu, V.V., Tapinos, N., Lulla, R.R., and El-Deiry, W.S. "Potent preclinical sensitivity to imipridone-based combination therapies in oncohistone H3K27M-mutant diffuse intrinsic pontine glioma is associated with induction of the integrated stress response, TRAIL death receptor DR5, reduced ClpX and apoptosis," submitted, 2021). EPZ-6438 was purchased from Selleckchem and was solubilized in DMSO at a storage concentration of 20 mM. PF-06821497 was purchased from ChemieTek and was solubilized in DMSO at a storage concentration of 10 mM. Vorinostat was purchased from MedKoo Biosciences and was solubilized in DMSO at a storage concentration of 50 mM. ONC201 was supplied by Oncocotics, Inc and reconstituted in DMSO at a storage concentration of 20 mM. Dopamine was purchased from Sigma-Aldrich and was solubilized in PBS at a storage concentration of 50 mM. Sumanirole was purchased from Sigma-Aldrich and was solubilized in PBS at a storage concentration of 20 mM.

Cell viability and apoptosis assays

Cells were seeded in opaque-walled 96-well plates at a density of 4000–5000 cells per well and incubated overnight in 100 μ L culture medium before addition of single-agent ONC201, vorinostat, EPZ-6438, PF-06821497, or the combination of ONC201 plus PF-06821497, ONC201 plus vorinostat, ONC201 plus EPZ-6438, vorinostat plus EPZ-6438, or ONC201, EPZ-6438, and vorinostat. Treatment was continued for 72 H. 20 μ L CellTiterGlo bioluminescence agent (Promega Corporation, Madison, WI) was added into each well. The content was mixed for 2 Min on a plate shaker to induce cell lysis. Cell viability was determined with the CellTiterGlo assay. Combination indices (CI) were calculated by the method of Chou and Talalay using the CompuSyn software. CI < 1.0 indicates drug synergy.

Sub-G1 analyses were performed to quantify apoptosis. Cells were seeded in 6-well plates at a density of 4×10^5 – 5×10^5 cells per well and incubated overnight in 2 mL culture medium before addition of single-agent ONC201, vorinostat, EPZ-6438, or the combination of ONC201 plus vorinostat, ONC201 plus EPZ-6438, vorinostat plus EPZ-6438, or ONC201, EPZ-6438, and vorinostat. After treatment of 72 H, the adherent cells were trypsinized, floating and adherent cells were fixed in 75% ethanol and stained with propidium iodide in the presence of pancreatic ribonuclease (RNase A). Sub-G1 analyses by flow cytometry were performed using a Coulter-Beckman Elite Epics cytometer.

Immunoblotting

Cells were seeded in 6-well plates at a density of 4×10^5 – 5×10^5 cells per well or 12-well plates at a density of 2×10^5 – 3×10^5 per well and incubated overnight in culture media before the addition of single-agent ONC201, vorinostat, EPZ-6438, PF-06821497, or the combination of ONC201 plus PF-06821497, ONC201 plus vorinostat, ONC201 plus EPZ-6438, vorinostat plus EPZ-6438, or ONC201, EPZ-6438, and vorinostat. After treatment for 48 H, the cells were washed with PBS and lysed in lysis buffer [150 mM NaCl, 1% Triton X-100, 0.5% Sodium deoxycholate, 0.1% SDS, 50mM Tris-HCl (pH8.0)]. The proteins were quantified with the Bio-Rad protein assay. LDS Sample Buffer (4x) and reducing reagent were added into the lysates. For the immunoblotting of histone, the cells were treated for 72 H and lysed directly with lysis buffer [150 mM NaCl, 1% Triton X-100, 0.5% Sodium deoxycholate, 0.1% SDS, 50mM Tris-HCl (pH8.0)] plus LDS Sample Buffer (4X). The lysates were loaded equally onto 4 to 12% NuPAGE SDS-polyacrylamide gels (Thermo Fisher Scientific). Standard procedures were performed to transfer proteins to polyvinylidene difluoride (PVDF) membranes. After blocking with 5% milk, the PVDF membranes were incubated with primary antibody overnight and subsequently appropriate secondary antibodies labeled with horseradish peroxidase for 1 H. The membranes were developed using an ECL reagent. The primary antibodies used in this study were as follows: antibodies against PARP (cat. no. 9542S), cleaved-caspase 3 (clvd-caspase 3, cat. no. 9661S), ATF4 (cat. no. 11815S), CHOP (cat. no. 2895S), DR5 (cat. no. 3696S), DRD2 (cat. No sc5303), Acetyl Histone H3 (Lys27) Antibody (cat. no. 4353S) (Cell Signaling), Histone H3 (tri-methyl K27) antibody (mAbcam 6002), and Histone H3 antibody (cat. no. 9715s). Secondary antibodies were acquired from Pierce (cat. nos. 31430 and 31460) (horseradish peroxide-conjugated).

Quantitative Reverse-Transcription Polymerase Chain Reaction (qRT-PCR)

Cells were seeded in 6-well plates at a density of 4×10^5 – 5×10^5 cells per well and incubated overnight in culture media before the addition of single-agent ONC201, vorinostat, or the combination of ONC201 plus vorinostat. Treatment was continued for 24 H. RNA was extracted using the RNeasy Plus Mini Kit (Qiagen) according to manufacturers' instructions

and quantitated using a Nanodrop spectrophotometer. Genes of interest were amplified using 2 μ g of total RNA reverse-transcribed to cDNA using a Superscript II kit (Invitrogen) with random hexamer primer. In the real-time PCR step, PCR reactions were performed in triplicate with 1 μ L cDNA/20 μ L reaction and primers specific for DRD1, DRD2, DRD3, DRD5, and glyceraldehyde-3-phosphate dehydrogenase (GAPDH) using the ViiA 7 Real-Time PCR System (Applied Biosystems). Thermal cycling was initiated at 95°C for 10 Min followed by 40 cycles of PCR (95°C for 15 S and 60°C for 1 Min). GAPDH was used as an endogenous control, and vehicle control was used as a calibrator. The sequences of the primers are listed in Table S1. The basal expression of genes is depicted by Δ Ct. Ct represents the threshold cycle number. The relative changes in gene expression were calculated using the following formula: fold change in gene expression, $2^{-\Delta\Delta Ct} = 2^{-[\Delta Ct(T) - \Delta Ct(NT)]}$, T represents treatment samples, NT represents no-treatment control samples.

Transient knockdown using siRNA

Cells were plated in an antibiotic-free medium with 10% FBS in a 24-well plate and incubated overnight. siRNA (a pool of three target-specific siRNAs) (Santa Cruz Biotechnology) (10 nM final concentration) was transfected into cells using 1.5 μ L Lipofectamine RNAiMax. After 24 H, single-agent ONC201, EPZ-6438, or the combination of ONC201 plus EPZ-6438, vorinostat plus EPZ-6438, or ONC201, EPZ-6438, and vorinostat were added.

Cells for cell viability assessment were plated in antibiotic-free medium with 10% FBS in a 6-well plate and incubated overnight. siRNA (a pool of three target-specific siRNAs) (Santa Cruz Biotechnology) (10 nM final concentration) was transfected into cells using 7.5 μ L Lipofectamine RNAiMax. The Hep3B cell line was trypsinized after treatment with siRNA for 24 H and the AGS cell line was trypsinized after treatment with siRNA for 48 H and seeded in 96-well plates at a density of 5000 cells per well and incubated overnight in 100 μ L culture medium before drug treatment.

Results

EZH2 inhibitor EPZ-6438 or PF-06821497 synergizes with ONC201 and suppresses the cell viability of multiple cancer cell lines

To test our hypothesis that reduced H3K27 methylation would mimic H3K27M mutation associated with ONC201 sensitivity in glioma and confer sensitivity to other tumor types, we assessed the therapeutic effect of ONC201 alone or in combination with EZH2 inhibitors, EPZ-6438 or PF-06821497 *in vitro*. We quantitatively analyzed the combinatorial effects of EZH2 inhibitors with ONC201. The data showed that EZH2i EPZ-6438 synergizes with ONC201 to suppress the cell viability of breast cancer and GBM cells *in vitro* (Fig. 1A, 1B, Table S2). Treatment with EPZ-6438 leads to a shift of ONC201 IC50 (Fig. S1A). The synergy between ONC201 and EPZ-6438 was observed in ER+/PR+/Her2+ breast cancer cell line MCF7, ER+/PR-/Her2+ breast cancer cell line MDA-MB-361 (Fig. 1A, 1B, Table S2), and triple-negative breast cancer cell line MDA-MB-468 (Fig. S1A, Table S2). The synergy was also observed in the U251 GBM cell line (Fig. 1A, 1B, Table S2) and the AGS gastric adenocarcinoma cell line (Fig. S1A, Table S2), although the synergy observed with AGS cells is less pronounced. We also observed that another EZH2i, PF-06821497 synergizes with ONC201 to suppress the cell viability of GBM cell line U251, DMG cell line SF8628, colorectal adenocarcinoma cell line HT29, pancreatic cancer cell line BxPC3, and ER+/PR-/Her2+ breast cancer cell line MDA-MB-361 (Fig. 1C, 1D, Table S3).

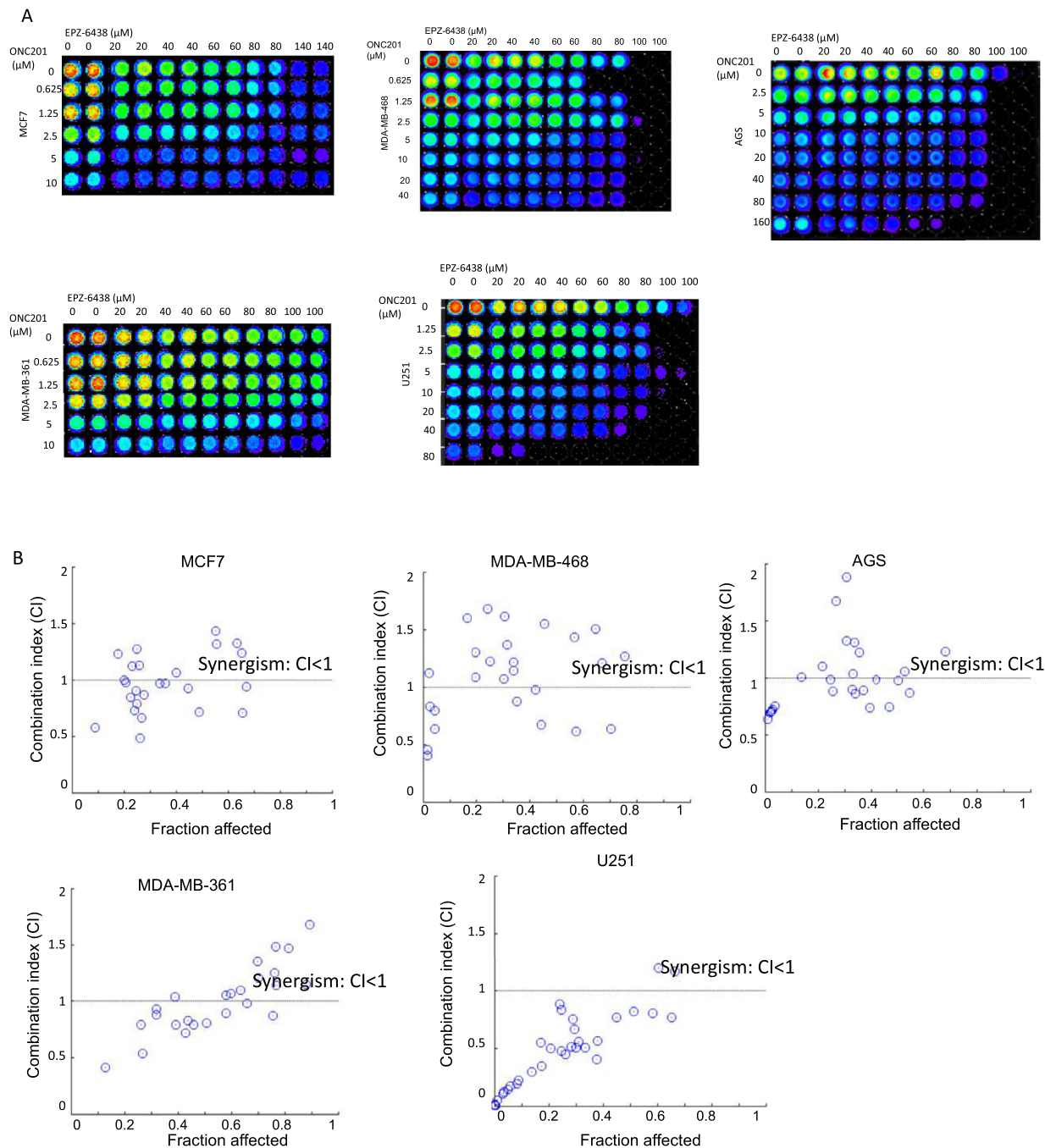


Fig. 1. Synergistic interaction between EZH2i and ONC201 in the suppression of cell viability of tumor cell lines. (A) CellTiterGlo assay (CTG) analysis of the viability of tumor cell lines treated with EPZ-6438 and ONC201 for 72 H. Drug doses and cell lines are as indicated. (B) The plot of the combination index (CI) as a function of cell viability for tumor cell lines treated with EPZ-6438 and ONC201 combinations in tested tumor cell lines. (C) CTG analysis of the viability of tumor cell lines treated with PF-06821497 and ONC201 for 72H. Drug doses and cell lines are as indicated. (D) The plot of the combination index (CI) as a function of cell viability for tumor cell lines treated with PF-06821497 and ONC201 combinations in tested tumor cell lines.

EZH2 inhibitors synergize with ONC201 to induce apoptosis

We further evaluated the effect of ONC201 in combination with an EZH2 inhibitor on tumor cell death induction. Immunoblotting detected cleaved-PARP and confirmed that EPZ-6438 or PF-06821497 synergizes with ONC201 to promote cancer cell apoptosis. We treated the tumor cell lines with single agent of ONC201, EPZ-6438, PF-06821497, ONC201 plus EPZ-6438, or ONC201 plus PF-06821497 for 48 H. The single treatment of ONC201 induced PARP cleavage in MCF7 (Fig. 2A, 2B), U251

(Fig. 2C, 2D), Hep3B (Fig. 5C, 5D), and Saos2 (Fig. S4A, S4B) cell lines, but not in MDA-MB-361 (Fig. S2A, S2B), AGS (Fig. S4C), or MM1 cell lines (Fig. S4D, S4E). The combination of ONC201 and EPZ-6438 induced more cleaved-PARP in MCF7 (Fig. 2A, 2B), U251 (Fig. 2C, 2D), Hep3B (Fig. 5C, 5D), MDA-MB-361 (Fig. S2A, S2B), Saos2 (Fig. S4A, S4B), and MM1S (Fig. S4D, S4E) cell lines, but not in AGS cells (Fig. S4C). In U251 cells, the combined treatment of PF-06821497 plus ONC201 also induced more cleaved-PARP (Fig. 2G). Thus, the mechanism of tumor suppression induced by ONC201 and combination of ONC201 and EZH2i in AGS is

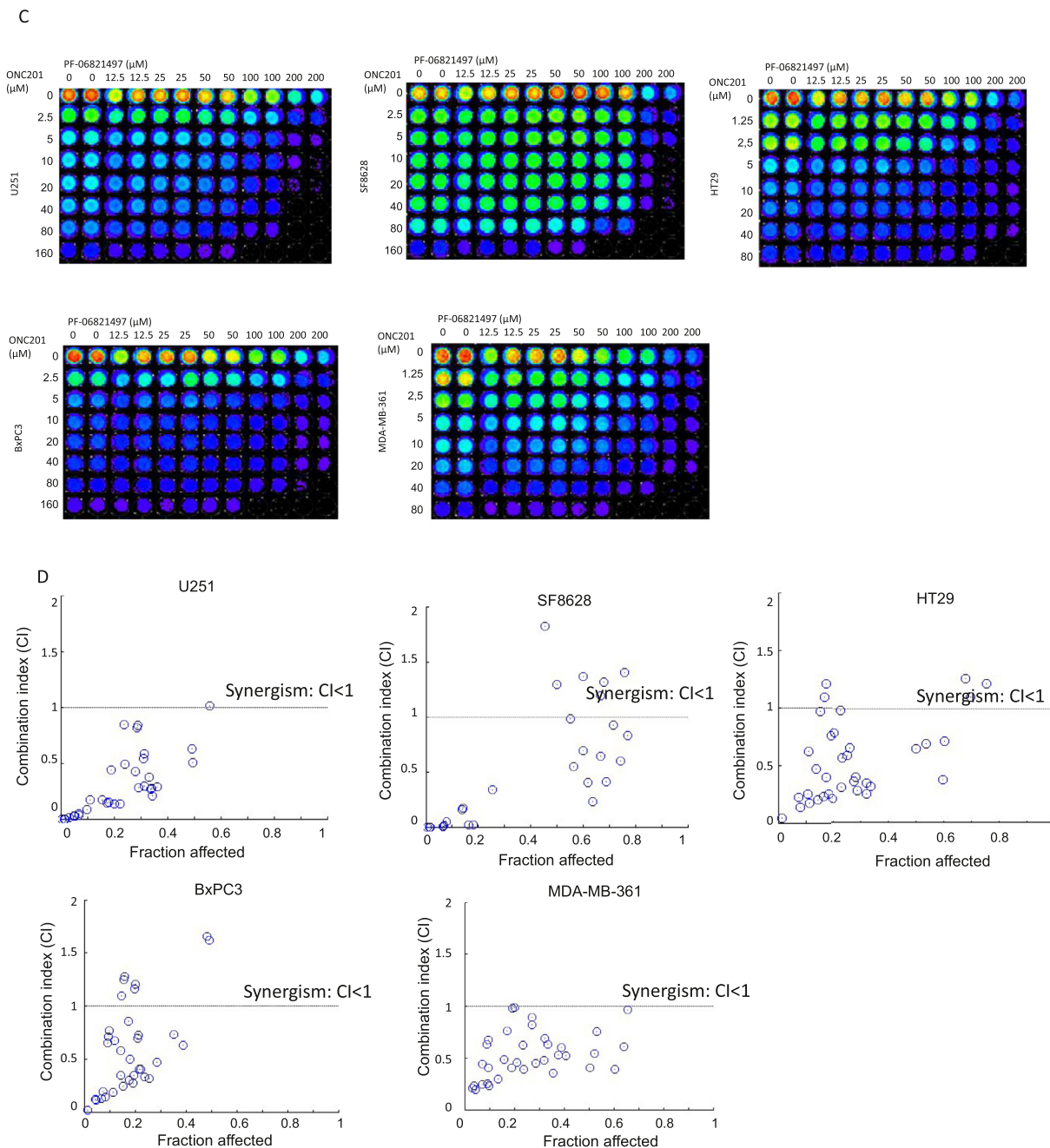


Fig. 1. Continued

different from that in other cell lines. Cleaved-caspase3 was induced by the combination of EPZ-6438 and ONC201 in Saos2 as well as in U251 treated with PF-06821497 plus ONC201 (Fig. S4, Fig. 2G). The sub-G1 analysis detected more apoptosis induced by the combination of ONC201 and EPZ-6438 as compared with single agents in the MDA-MB-468 (Fig. 2F) and MCF7 (Fig. S2E) cell lines.

EPZ-6438 synergizes with ONC201 and triggers an integrated stress response and TRAIL pathway to promote cell death and apoptosis

ONC201 kills tumor cells by triggering an integrated stress response dependent on ATF4 activation [1]. Activating transcription factor-4 (ATF4)

is the master coordinator of the integrated stress response (ISR), which can promote cell death [25]. We treated the cancer cell lines with a single-agent of ONC201, EPZ-6438, PF-06821497, or ONC201 plus EPZ-6438, ONC201 plus PF-06821497 for 48 hr. Immunoblotting detected more induction of ATF4 in cells treated with the combination of ONC201 and EPZ-6438 as compared with treatment with a single-agent in the MCF7 (Fig. 3A, 3B), U251 (Fig. 3D, 3E), MDA-MB-361 (Fig. S3A, S3B), and Saos2 (Fig. S5B) cell lines and also in U251 treated with the combination of ONC201 and PF-06821497 (Fig. 3G, 3H). ATF4 promoted apoptosis, in part, by regulating the expression of CHOP [26]. CHOP induces death receptor DR5, that plays a role in the induction of apoptosis under ER stress [27]. The ISR induced by ONC201 triggers an increase of TRAIL and DR5. CHOP and DR5 expression increase in response to exposure to

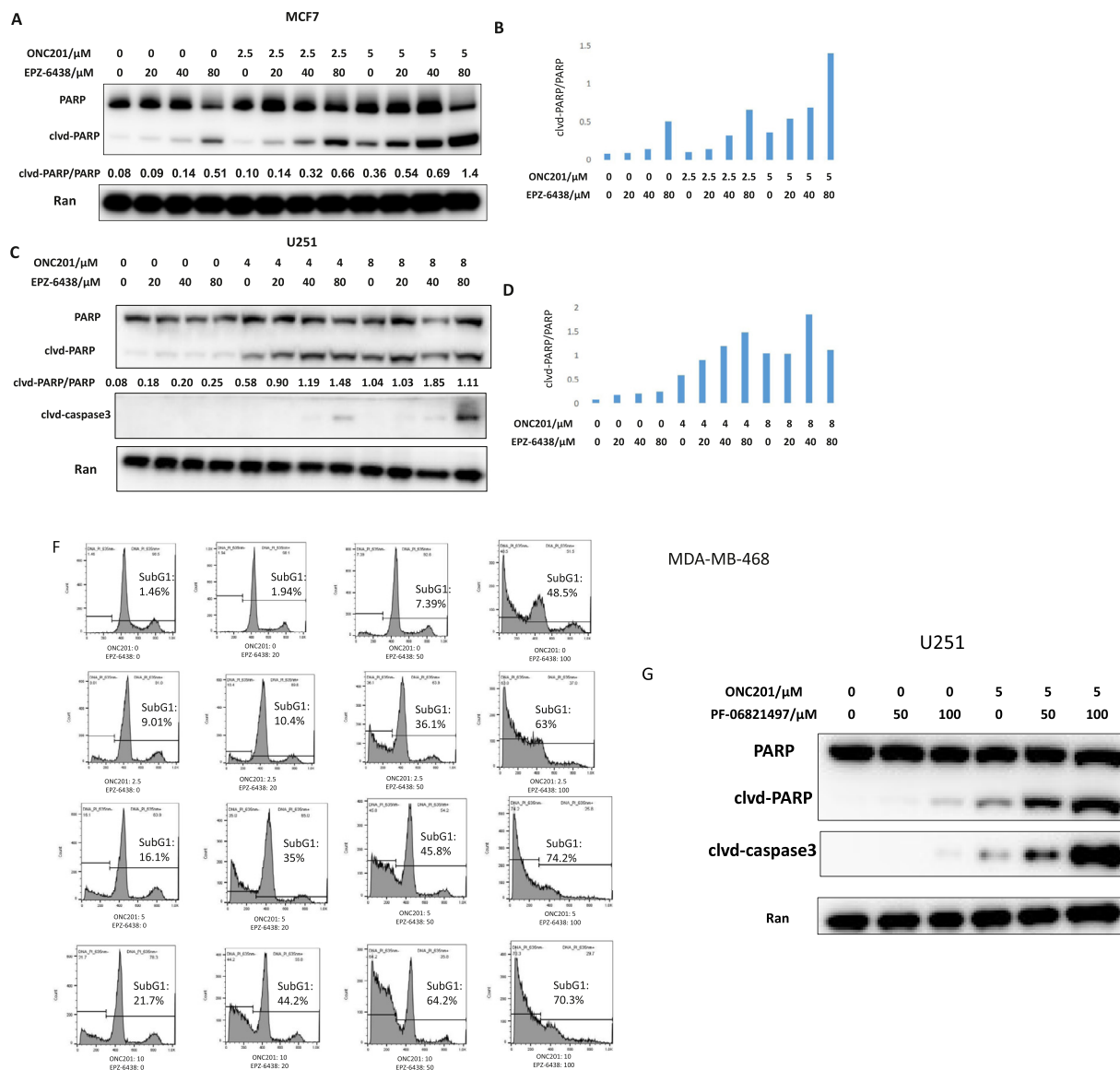


Fig. 2. Combination of EZH2i plus ONC201 enhances tumor cell line apoptosis. Immunoblotting of cleaved-PARP (clvd-PARP) in (A) MCF7 treated with EPZ-6438 (0, 20, 40, 80 μ M) plus ONC201 (0, 2.5, 5 μ M) and (C) U251 treated with EPZ-6438 (0, 20, 40, 80 μ M) plus ONC201 (0, 4, 8 μ M) for 48 H. Densitometric analysis of clvd-PARP/PARP ratios is as indicated in (B) for MCF7 and (D) for U251. (F) Flow cytometric analysis of cell death distribution of MDA-MB-468 cell lines treated with EPZ-6438 (0, 20, 50, 100 μ M) plus ONC201 (0, 2.5, 5, 10 μ M) for 72 H. The observed % sub-G1 fraction for each experimental condition is as indicated. (G) Immunoblotting of cleaved-PARP (clvd-PARP) and cleaved-caspase 3 in U251 treated with PF-06821497 (0, 50, 100 μ M) plus ONC201 (0, 5 μ M).

ONC201 in cultured HCT116 cells [1]. However, no induction of CHOP is detected after 48 H of treatment of either single-agent of ONC201 or ONC201 plus EPZ-6438 in MCF7 (Fig. S3C). Immunoblotting detected more induction of DR5 in MCF7 (Fig. 3A, 3C) and U251 (Fig. 3D, 3F) cells treated with the combination of ONC201 and EPZ-6438 or ONC201 plus PF-06821497 as compared with treatment with a single-agent (Fig. 3G, 3I). Up-regulation of ATF4 and DR5 suggests an involvement of the ISR and TRAIL pathway in apoptosis induced by ONC201 or a combination of ONC201 and EZH2i in human glioma cells without H3K27M mutation. Knockdown of ATF4 (Fig. 7C) reduced DR5 induction (Fig. 7D, 7E), cell viability suppression (Fig. 7A, 7B), and apoptosis (Fig. 7D, 7F) induced by the single-agent of ONC201 or the combination of ONC201 and EPZ-6438 in U251 glioma cells without H3K27M mutation. Thus, induction of ISR mediated the apoptosis induced by the combination of ONC201

and EPZ-6438 in U251 cells. Single treatment of ONC201 induced ATF4 and DR5 in Hep3B cells (Fig. 6D-6F). However, the addition of EPZ-6438 did not enhance the induction of ATF4 (Fig. 6D-6F). Knockdown of ATF4 in Hep3B appeared to induce greater cell viability suppression (Fig. 6SA, 6SB) and apoptosis (Fig. 6C), although the ATF4 knockdown reduced DR5 induction (Fig. 6C). Thus, the cell death induced by the combination of ONC201 and EPZ-6438 in Hep3B depends on the mechanism other than ISR or TRAIL pathway.

EPZ-6438 and HDAC inhibitor vorinostat synergize with ONC201 and suppress cell viability of multiple cancer cell lines

EZH2i reduces global histone H3K27 methylation while HDACi induces histone acetylation and a more relaxed chromosome structure.

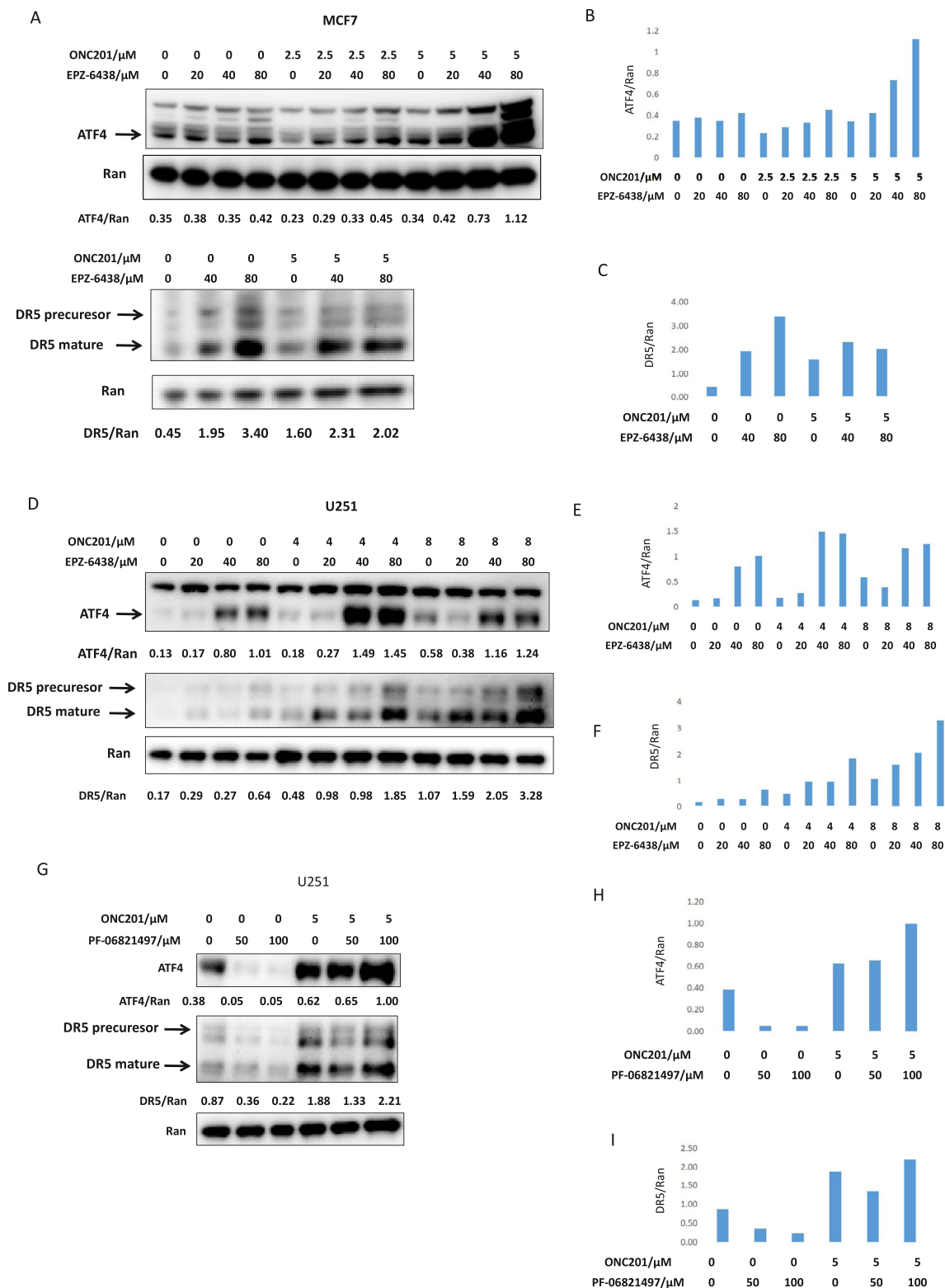


Fig. 3. The combination of EZHi and ONC201 enhances the up-regulation of AFT4 and DR5 induced by ONC201. (A) Immunoblotting of ATF4 and DR5 in MCF7 treated with EPZ-6438 (0, 20, 40, 80 μM) plus ONC201 (0, 2.5, 5 μM). Densitometric analysis of ATF4/Ran and DR5/Ran ratios in MCF7 is as indicated in (B) and (C). (D) Immunoblotting of ATF4 and DR5 in U251 treated with EPZ-6438 (0, 20, 40, 80 μM) plus ONC201 (0, 4, 8 μM) for 48 H. Densitometric analysis of ATF4/ran and DR5/Ran ratios in U251 is as indicated in (E) and (F).

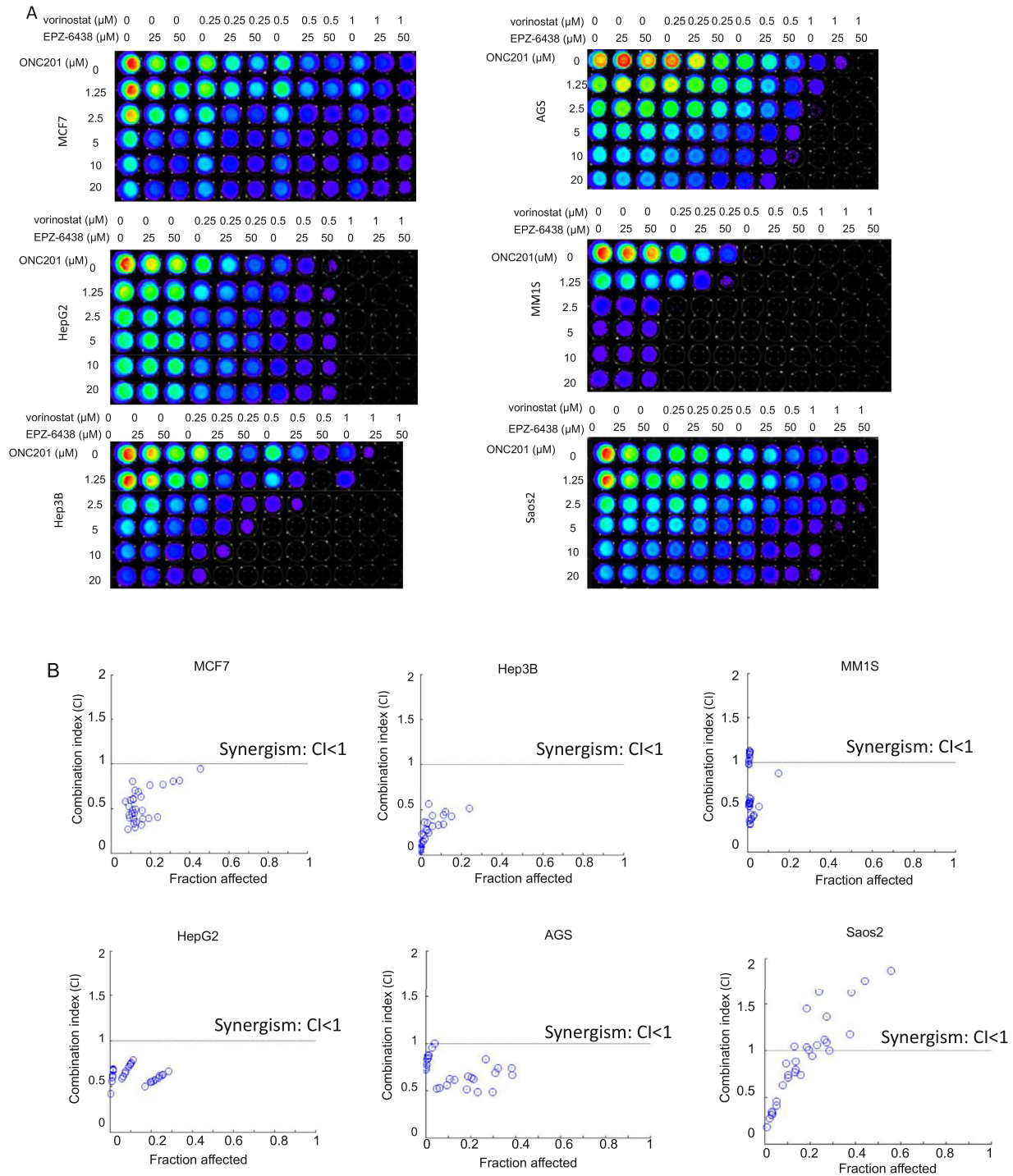


Fig. 4. The combination of EPZ-6438, vorinostat and, ONC201 is synergistic in the suppression of cell viability in multiple human tumor cell lines. (A) CTG analysis of cell viability of tumor cell lines treated with the combination of EPZ-6438, vorinostat, and ONC201 for 72 H. Cell line and drug doses are as indicated. (B) The plot of the combination index (CI) as a function of cell viability for tumor cell lines treated with the combination of EPZ-6438, vorinostat, and ONC201.

Both acetylation and reduction of methylation of histones lead to the de-repression of target gene transcription. We added the HDACi vorinostat to the combination of EPZ-6438 and ONC201 to evaluate the synergy of the three agents. The combination of the three agents appeared synergistic in breast cancer, hepatocellular carcinoma, gastric adenocarcinoma, multiple

myeloma, and osteosarcoma cell lines (Fig. 4A, 4B, Table S4). In MCF7, Hep3B and HepG2 cells, the combination of the three agents induced synergy at all the dosages use, and most of the combination index values ranged from 0.27-0.80 in MCF7 and 0.06-0.70 in HepG2 and Hep3B cells (Fig. 4A, 4B, Table S4).

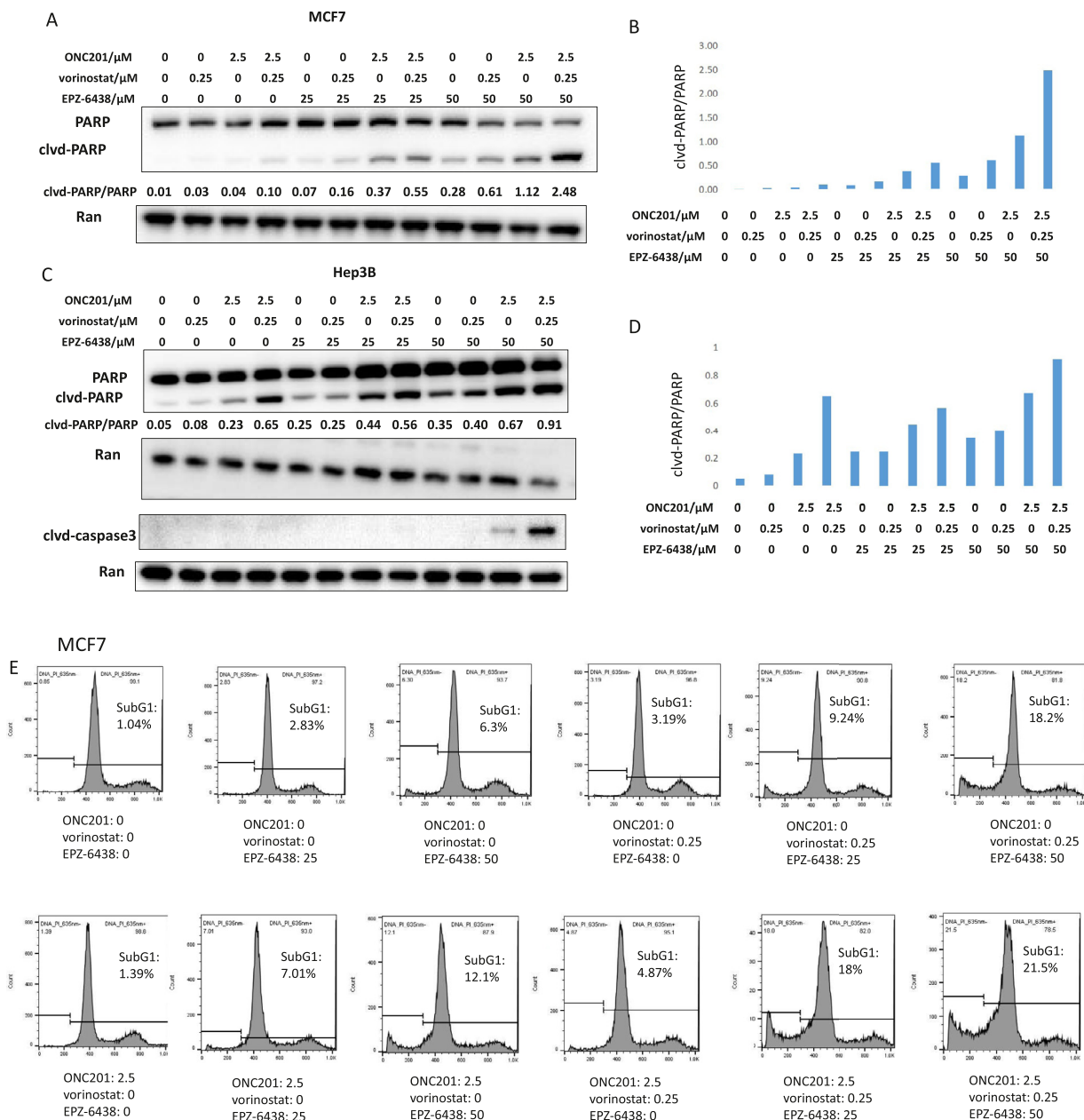


Fig. 5. The combination of EPZ-6438, vorinostat and ONC201 enhances apoptosis in human tumor cell lines. Immunoblotting of clvd-PARP in (A) MCF7 treated with the combination of EPZ-6438 (0, 25, 50 μ M), vorinostat (0, 0.25 μ M) and ONC201 (0, 2.5 μ M), and (C) Hep3B treated with EPZ-6438 (0, 25, 50 μ M), vorinostat (0, 0.25 μ M) and ONC201 (0, 2.5 μ M) for 48 H. Densitometric analysis of clvd-PARP/PARP ratios is as indicated in (B) for MCF7 and (D) for U251. (E) Flow cytometric analysis of cell death distribution of the MCF7 cell line treated with combination of EPZ-6438 (0, 25, 50 μ M), vorinostat (0, 0.25 μ M) and ONC201 (0, 2.5 μ M) for 72 H. The observed % sub-G1 fraction for each experimental condition is as indicated.

EPZ-6438 and vorinostat synergize with ONC201 to induce apoptosis

We further investigated the effects of the combination of EPZ-6438, vorinostat, and ONC201 on apoptosis. Immunoblotting of cleaved-PARP detected apoptosis induced by the combination of EPZ-6438, vorinostat, and ONC201 in MCF7 (Fig. 5A, 5B), Hep3B (Fig. 5C, 5D), Saos2 (Fig. S4A, S4B), and MM1S cell lines (Fig. S4D, S4E). The apoptosis was also demonstrated by the immunoblotting of cleaved-caspase 3 in Hep3B (Fig. 5C) and Saos2 cell line (Fig. S4A). But no apoptosis was detected in AGS cells (Fig. S4C). A Flow cytometry analysis of cell distribution of the MCF7 cell line treated with EPZ-6438, vorinostat, and ONC201 for 72 H

demonstrated the apoptosis induced by a combination of the three agents (Fig. 5E).

Role of integrated stress response and TRAIL pathway activation in the synergy of EPZ-6438 and vorinostat

We further investigated the mechanism of synergy with ONC201 and the epigenetic modulators by examining the integrated stress response mediator ATF4. Immunoblotting of ATF4 demonstrated that the combination of ONC201, vorinostat, and EPZ-6438 enhanced the induction of ATF4 and DR5 in MCF7 (Fig. 6A, 6B). The up-regulation of ATF4 implicates the ISR

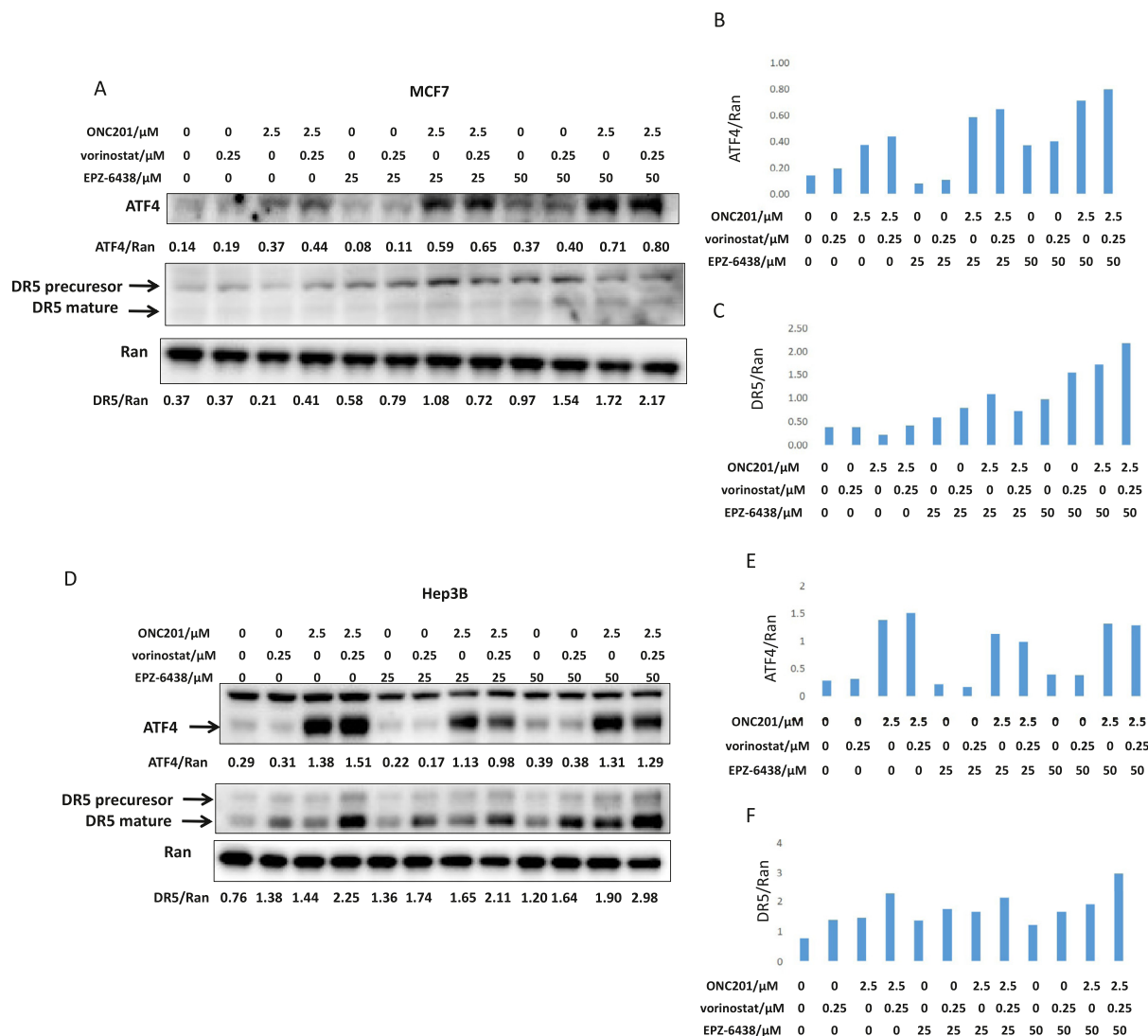


Fig. 6. EPZ-6438 and vorinostat enhance expression of ATF4 and DR5 induced by ONC201 in MCF7 and Hep3B cells. Immunoblotting of ATF4 and DR5 in MCF7 (A) and Hep3B (C) cells treated with the combination of EPZ-6438 (0, 25, 50 μ M), vorinostat (0, 0.25 μ M) and ONC201 (0, 2.5 μ M) for 48 H. Densitometric analysis of ATF4/Ran and DR5/Ran ratios in MCF7 is as indicated in (B) and (C) and Hep3B in (E) and (F).

in the apoptosis induced by the combination of ONC201, vorinostat, and EPZ-6438 in MCF7. In AGS and MM1S cell lines, no induction of ATF4 was detected with either the combination of ONC201, vorinostat, and EPZ-6438 or the single-agent of ONC201 (Fig. S5A, S5C). The single-agent of ONC201 appeared to reduce ATF4 in the AGS cell line (Fig. S5A). In Saos2, EPZ-6438 enhanced ATF4 induction, but the addition of vorinostat reduced the up-regulation of ATF4 (Fig. S5B). In Hep3B, although ONC201 alone could induce ATF4, the addition of vorinostat or EPZ-6438 appeared to reduce the expression of ATF4 in the Hep3B cell line under the experimental conditions (Fig. 6D, 6E). Knockdown of ATF4 induced more cell viability suppression (Fig. S6A, S6B) and more apoptosis detected by immunoblotting of PARP cleavage and caspase 3 cleavage (Fig. S6C) in Hep3B treated with the combination of the three agents. ATF4 knockdown had no stable impact on the viability suppression induced by the combination of ONC201, EPZ-6438, and vorinostat in AGS cells (Fig. S6D, S6E). Thus, the induction of the ISR contributed to the apoptosis induced by the combination of the 3 agents in MCF7 cell line. In U251 DR5 induction appears dependent upon ATF4 induction and the increase in DR5 correlates with ONC201-,

EPZ-6438- or combination therapy-induced cell death as measured by PARP cleavage (Fig. 7). ATF4 is induced in Saos2 after treatment with ONC201 or combinations of ONC201 with EPZ-6438 (Fig. S5B). In some cell lines such as AGS, MM1S, and Hep3B, there may be other mechanisms that contribute to the synergy with the epigenetic modulators and ONC201, although the western blot data in Figure S5 is performed at 48 hours after drug treatment. Nonetheless, the knockdown of ATF4 in Hep3B did not reduce apoptosis after ONC201 treatment (Fig. S6).

EPZ-6438 reduces methylation at H3K27 in multiple cancer cell lines

To validate the epigenetic modulation of H3K27 as a molecular mimic of H3K27M that is associated with ONC201 sensitivity, we examined the methylation changes at H3K27 in EZH2i- and ONC201-treated tumor cells. We treated MCF7 and U251 with a single-agent of EPZ-6438, ONC201, or EPZ-6438 plus ONC201 and U251 with a single-agent of PF-06821497, ONC201, or PF-06821497 plus ONC201 for 72 hours. Immunoblotting showed that EPZ-6438 reduces H3K27 tri-methylation in

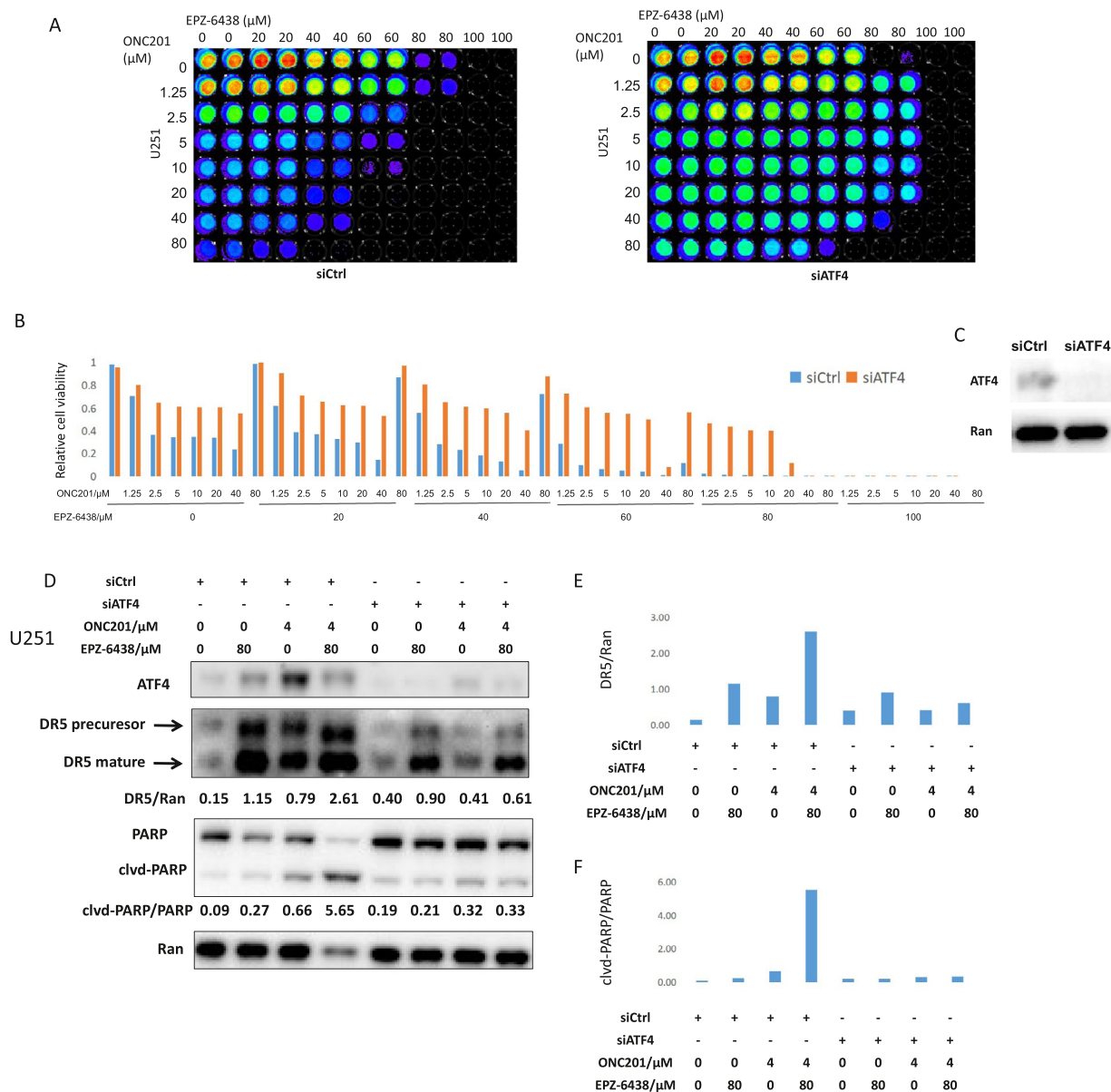


Fig. 7. Knock-down of ATF4 reduces cell death induced by the combination of ONC201 and EPZ-6438 in U251 glioma cells that do not harbor an H3K27M mutation. (A) CellTiterGlo assay (CTG) analysis of cell viability in U251 cells treated with the combination of EPZ-6438 and ONC201 for 72 hours after ATF4 knockdown. (B) Cell viability assessment of U251 cells treated with the combination of EPZ-6438 and ONC201 for 72 H after ATF4 knockdown. (C) ATF4 was knocked down in U251 for cell viability assessment. (D) Immunoblotting of ATF4, DR5 and clvd-PARP in U251 treated with the combination of EPZ-6438 and ONC201 for 72 H after ATF4 knockdown. Densitometric analysis of DR5/Ran and clvd-PARP/PARP ratios in U251 cells is as indicated in (E) and (F).

the MCF7 (Fig. 8B, S7A), Hep3B (Fig 8C), and U251 (Fig. 8A) cell lines, PF-06821497 reduced H3K27 tri-methylation in U251 cells (Fig. S7D). We treated the MCF7, MM1S, and Hep3B cell lines with a single-agent of EPZ-6438, vorinostat, or ONC201 or the combination of the three agents for 72 H. Immunoblotting detected reduced H3K27 tri-methylation with the treatment of EPZ-6438 or the combination of EPZ-6438 and vorinostat (Fig. 8B, 8C, Fig. S7B). Immunoblotting of Hep3B detected more H3K27 acetylation with the treatment of EPZ-6438 or the combination of EPZ-6438 and vorinostat (Fig. S7C). The epigenetic alteration induced by EPZ-6438, PF-06821497, or vorinostat may contribute to the synergy of the combination in the suppression of tumor cells.

mRNA expression of dopamine receptors is not associated with ONC201 sensitivity in the tested tumor cell lines either before or after drug treatment by epigenetic drugs

ONC201 is a selective antagonist of the dopamine D2-like receptors, specifically, DRD2 and DRD3. DRD5 is a D1-like receptor that opposes DRD2 signaling, and we previously showed that a DRD5 antagonist synergizes with ONC201 [24]. A DRD2+DRD5- biomarker signature is associated with enhanced ONC201 tumor cell sensitivity in clinical specimens [23]. We hypothesized that the interaction between ONC201 and D2-like dopamine receptors plays a role in the anti-cancer effects of

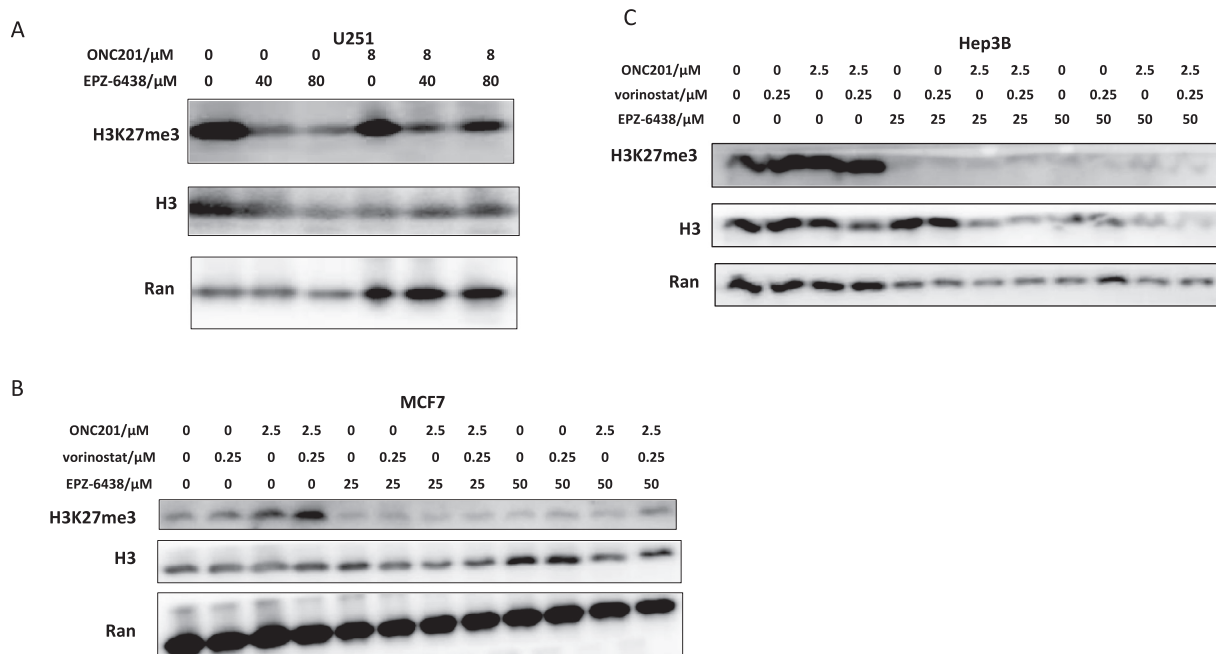


Fig. 8. Post-translational modification of H3K27 following treatment of tumor cells with EPZ-6438 or vorinostat. EPZ-6438 or EPZ-6438 plus vorinostat reduce H3K27 tri-methylation in (A) U251 cell lines treated with the combination of EPZ-6438 (0, 40, 80 μM) and ONC201 (0, 8 μM), (B) MCF7 cells treated with the combination of EPZ-6438 (0, 25, 50 μM), vorinostat (0, 0.25 μM), and ONC201 (0, 2.5 μM) and (C) Hep3B cells treated with the combination of EPZ-6438 (0, 25, 50 μM), vorinostat (0, 0.25 μM), and ONC201 (0, 2.5 μM) for 72 H.

Table 1

The expression of the different dopamine receptors is variable across different cell types. (ΔCt values Are Shown)

Cell Type	Cell Line	DRD1	DRD2	DRD3	DRD5
Colorectal cancer	HCT116	10.7	17.9	17.1	18.1
	HT29	9.9	9.5	13.1	12.4
	SW480-1	9.3	3.2	7.0	6.7
Breast cancer	MCF7	5.1	6.4	13.2	11.9
	MDA-MB-361	11.3	11.8	17.4	15.3
	MDA-MB-468	12.2	5.7	12.0	12.5
Glioblastoma	T98G-1	14.4	1.1	12.0	12.4
	SF8628	ND	11.0	14.8	13.7
	U251	9.9	0.8	16.4	13.0
Gastric cancer	SNU16-1	8.0	ND	ND	8.3
Prostate cancer	DU145	12.7	14.9	12.8	13.5
	PC3	15.0	13.7	13.2	14.0

ND = not detected.

ONC201, and thus, the basal expression of dopamine receptors and the ratios of D2-like versus D1-like dopamine receptors expression may correlate with ONC201 sensitivity. We determined the basal expression of dopamine receptors in multiple tumor cell lines through RT-PCR and investigated the potential association between the levels of dopamine receptors and IC50 of ONC201. The basal mRNA expression of dopamine receptors was depicted by ΔCt (Table 1). In the 12 tumor cell lines tested, no correlation was detected between ONC201 sensitivity and basal mRNA expression of dopamine receptors or the ratio of DRD2 versus DRD5 expression (Fig. 9). We tried to modulate the expression of dopamine receptors with HDACi vorinostat and investigate whether modulation of dopamine receptors is associated with sensitization to ONC201. The relative changes in gene expression were depicted by $2^{-\Delta\Delta\text{Ct}}$. In the 11 tumor cell lines tested, no correlation was detected between changes of mRNA expression of dopamine

receptors and changes of IC50 of ONC201 caused by vorinostat treatment (Fig. 10).

Expression of DRD2 in tumor cells treated with the combination of epigenetic modulators and ONC201

To understand whether DRD2 plays a role in the synergy of the combination of epigenetic modulators and ONC201, we evaluated the impact of the combination of epigenetic modulators and ONC201 on the expression of DRD2 in the tumor cell lines at the protein level. The addition of the epigenetic modulators increased the expression of DRD2 in U251, MCF7 and AGS cells (Fig. S8). However, significant up-regulation of DRD2 expression was not observed in U251 (Fig. S8A, S8B). In MCF7 cells there was some apparent increase in DRD2 with EPZ-6438 (Fig S8C, S8D) and a

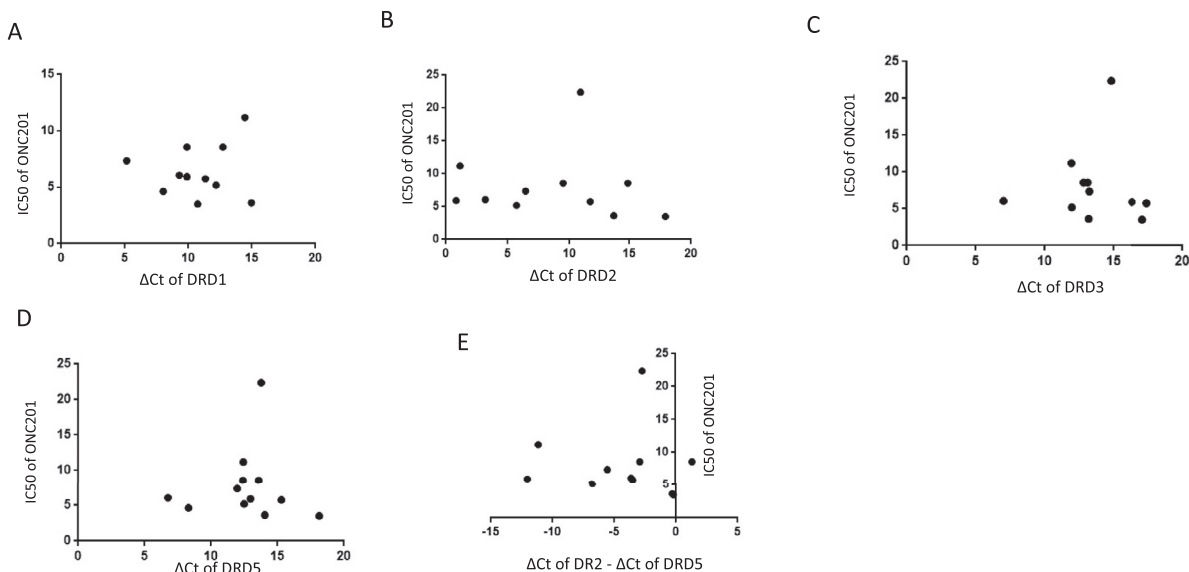


Fig. 9. ONC201 sensitivity is not associated with basal expression of dopamine receptors or with the ratio of DRD2/DRD5 in a panel of 12 tumor cell lines. (A–D) Lack of correlation between dopamine receptor expression (as indicated) determined by RT-PCR with ONC201 sensitivity in a panel of 12 human cancer cell lines. (E) The ratio of DRD2 expression versus DRD5 expression in multiple cancer cell lines. ΔCt was calculated by (Ct value of dopamine receptor - Ct value of GAPDH). The 12 cell lines are HCT116, HT29, SW480, MCF7, MDA-MB-361, MDA-MB-468, T98G, SF8628, U251, SNU16, DU145, and PC3 and the ΔCt values are shown in [Table 1](#).

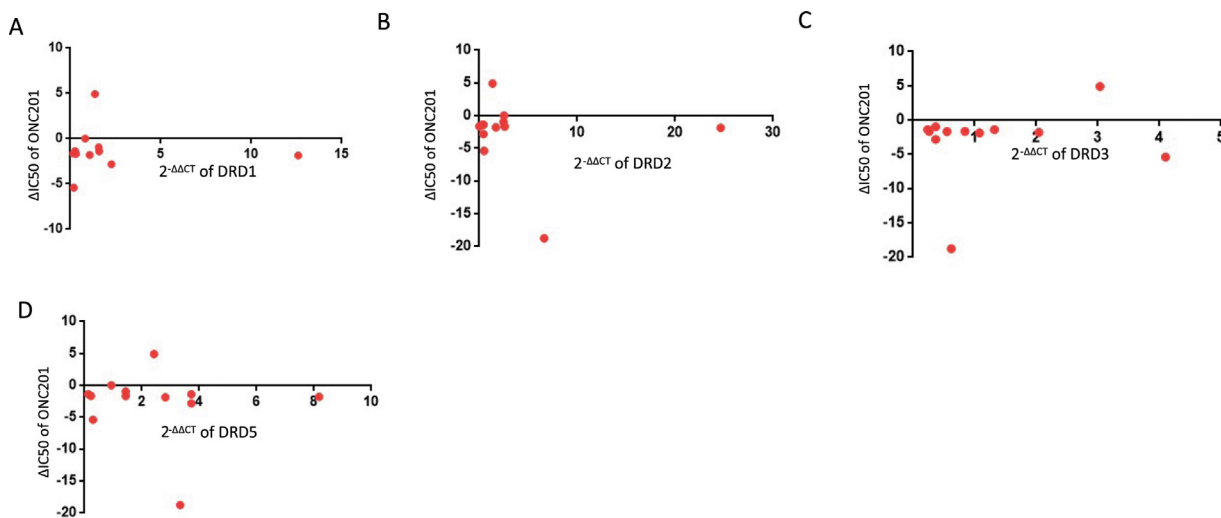


Fig. 10. Change of ONC201 sensitivity was not associated with modulation of dopamine receptor mRNA expression by vorinostat in multiple human tumor cell lines. The change of dopamine receptor mRNA expression was depicted by $2^{-\Delta\Delta\text{Ct}}$ and is shown for the 12-cell line panel as indicated. The 12 cell lines are HCT116, HT29, SW480, MCF7, MDA-MB-361, MDA-MB-468, T98G, SF8628, U251, SNU16, DU145, and PC3 and the ΔCt values are shown in [Table 1](#). ΔIC_{50} of ONC201 was generated by (IC₅₀ of ONC201 with simultaneous treatment of vorinostat - IC₅₀ of ONC201 without vorinostat treatment).

similar trend although less pronounced was observed in AGS cells (Fig. S8E, S8F). It remains unclear whether up-regulation of DRD2 may play a role in the synergistic effect of epigenetic modulators and ONC201 in some cell lines where DRD2 expression may be altered for example, by EPZ-6438.

Reduced H3K27me3 methylation in multiple tumor cell types including H3K27M-mutated DIPG cells treated with EPZ-6438 or vorinostat and ONC201

To further explore relationships between H3K27 methylation and acetylation with observed synergies between the epigenetic drugs EPZ-

6438 or vorinostat in combination with ONC201, we evaluated the H3K27 modifications and correlated the effects with apoptotic cell death (Fig. 11). In H3K27M-mutated DIPG-13 cells, we observed potent synergy between combinations of ONC201 plus either vorinostat or EPZ-6438 (Fig. 11A). The synergistic cell death noted with increase in PARP cleavage following treatment with ONC201 + vorinostat or ONC201 + EPZ-6438 or the triple combination correlated with reduced H3K27 methylation and no significant increase in H3K27 acetylation ((Fig. 11A). A similar pattern was noted in DIPG-25 cells with decreased H3K27 methylation with the ONC201 + epigenetic drug doublets or triple combination of ONC201 + EPZ-6438 + vorinostat (Fig. 11B). There was a modest increase

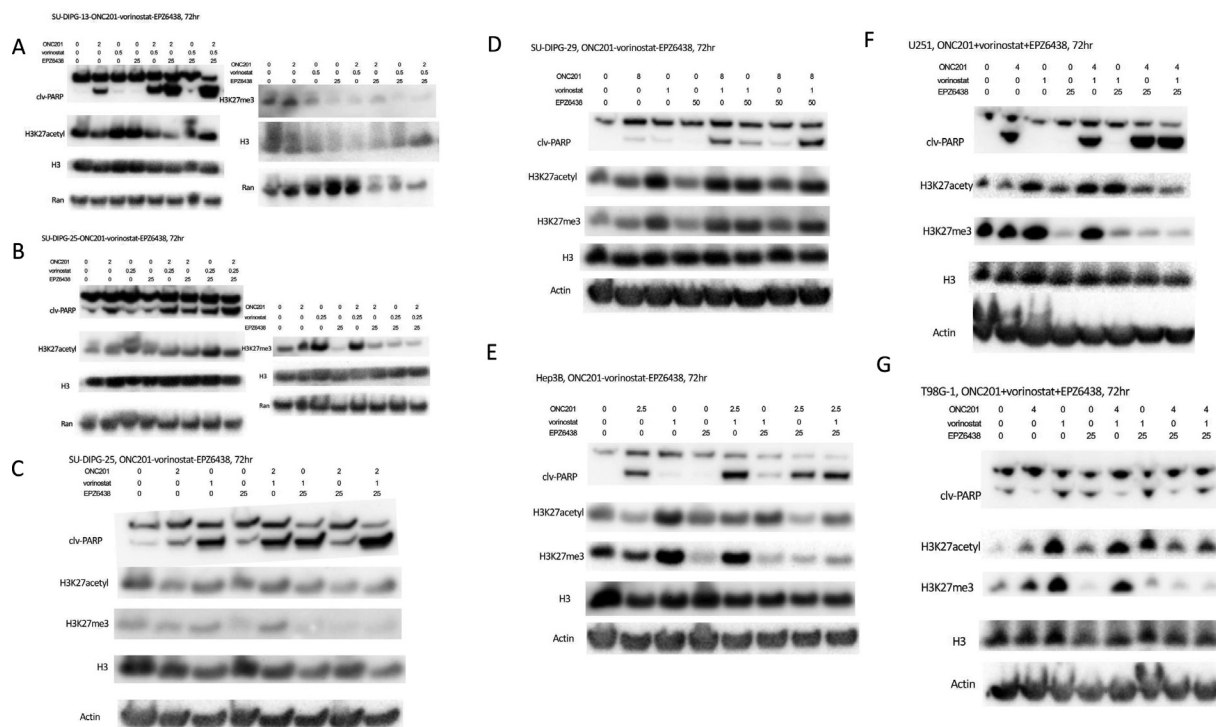


Fig. 11. Reduced H3K27me3 methylation in multiple tumor cell types including H3K27M-mutated DIPG cells treated with EPZ-6438 or vorinostat and ONC201. (A) H3K27M-mutated DIPG-13 cells were treated with combinations of ONC201 plus either vorinostat or EPZ-6438. PARP cleavage, H3K27 methylation and H3K27 acetylation is shown by western blot along with loading controls. (B) H3K27M-mutated DIPG-25 cells were treated with combinations of ONC201 plus either vorinostat or EPZ-6438. PARP cleavage, H3K27 methylation and H3K27 acetylation is shown by western blot along with loading controls. (C) A second experiment with H3K27M-mutated DIPG-25 cells were treated with combinations of ONC201 plus either vorinostat or EPZ-6438. PARP cleavage, H3K27 methylation and H3K27 acetylation is shown by western blot along with loading controls. (D–G). DIPG-29, Hep3B, U251, and T98G cells were treated with combinations of ONC201 plus either vorinostat or EPZ-6438. PARP cleavage, H3K27 methylation and H3K27 acetylation is shown by western blot along with loading controls.

in H3K27 acetylation and methylation with combinations containing vorinostat although methylation was suppressed with the triple combination (Fig. 11B). DIPG-25 cells showed a similar pattern of suppression in H3K27 methylation with EPZ-6438 plus ONC201 or the triple combination that included vorinostat (Fig. 11C). Despite the observed synergies, there were no significant increases observed in H3K27 acetylation in DIPG-25 cells with ONC201 in combination with the epigenetic drugs as compared to vorinostat alone at 72 H (Fig. 11C). An exception to H3K27 methylation suppression with ONC201 in combination with EPZ-6438 or vorinostat was noted in DIPG-29 cells undergoing apoptosis (Fig. 8D). Hep3B, U251, and T98G showed suppression of H3K27 methylation and appreciable increase in H3K27 acetylation with combinations of ONC201 plus EPZ-6438 or vorinostat or the triple combination in cells undergoing apoptosis (Fig. 11E, F, G).

Dopamine or the DRD2 agonist sumanirole do not rescue ONC201 mediated loss of cell viability in multiple human tumor cell lines including DIPG

Because we did not observe correlations between dopamine receptor DRD2 or DRD3 mRNA expression and loss of cell viability of multiple tumor cell lines treated with ONC201 alone or in combination with epigenetic drugs, we explored whether the addition of dopamine to the cultures might alter the results. Dopamine did not rescue apoptosis by ONC201 in different tumor cell lines (N=10) including 2 GBM, 3 DIPG (Fig. 12, 13) and did not prevent ATF4 induction, DR5 activation or

apoptosis (Fig. 15). DRD2 agonist sumanirole did not protect brain tumor cells (N = 6 including 4 DIPG cell lines) from ONC201 reduction in viability (Fig. 14). In experiments where we added dopamine to cell cultures, we confirmed an increase in phosphorylation of PKA substrate after ONC201 treatment and some suppression when dopamine was added, as another indicator that dopamine receptor signaling was engaged. Thus, experimentally in cell culture, dopamine or dopamine receptor DRD2 agonist sumanirole cannot overcome the functional activity of ONC201 to activate the cell death pathway in human cancer cell lines, including DIPG.

Discussion

ONC201 blocks cells from proliferating and kills tumors in cell and animal models. Multiple clinical trials of ONC201 in various cancer types have demonstrated the safety and preliminary efficacy of ONC201 in multipole tumor types. A subset of pediatric and adult patients with histone H3K27M-mutated midline glioma benefit from ONC201 [8, 9, 28]. EZH2 is a histone methyltransferase and EZH2i's reduce the bi- and tri-methylation on H3K27. We reasoned that inhibition of H3K37 methylation by an EZH2 inhibitor may mimic the H3K27M mutation and thus predicted and sought to demonstrate synergy from the combination of EZH2i with ONC201 in multiple tumor types.

We treated multiple tumor cell lines with the combination of EZH2i EPZ-6438/PF-06821497 and ONC201 and observed synergy of the two agents in breast cancer cell lines, including ER+/PR+/Her2+, ER+/PR-/Her2+, and triple-negative breast cancer, GBM, DMG, colorectal cancer,

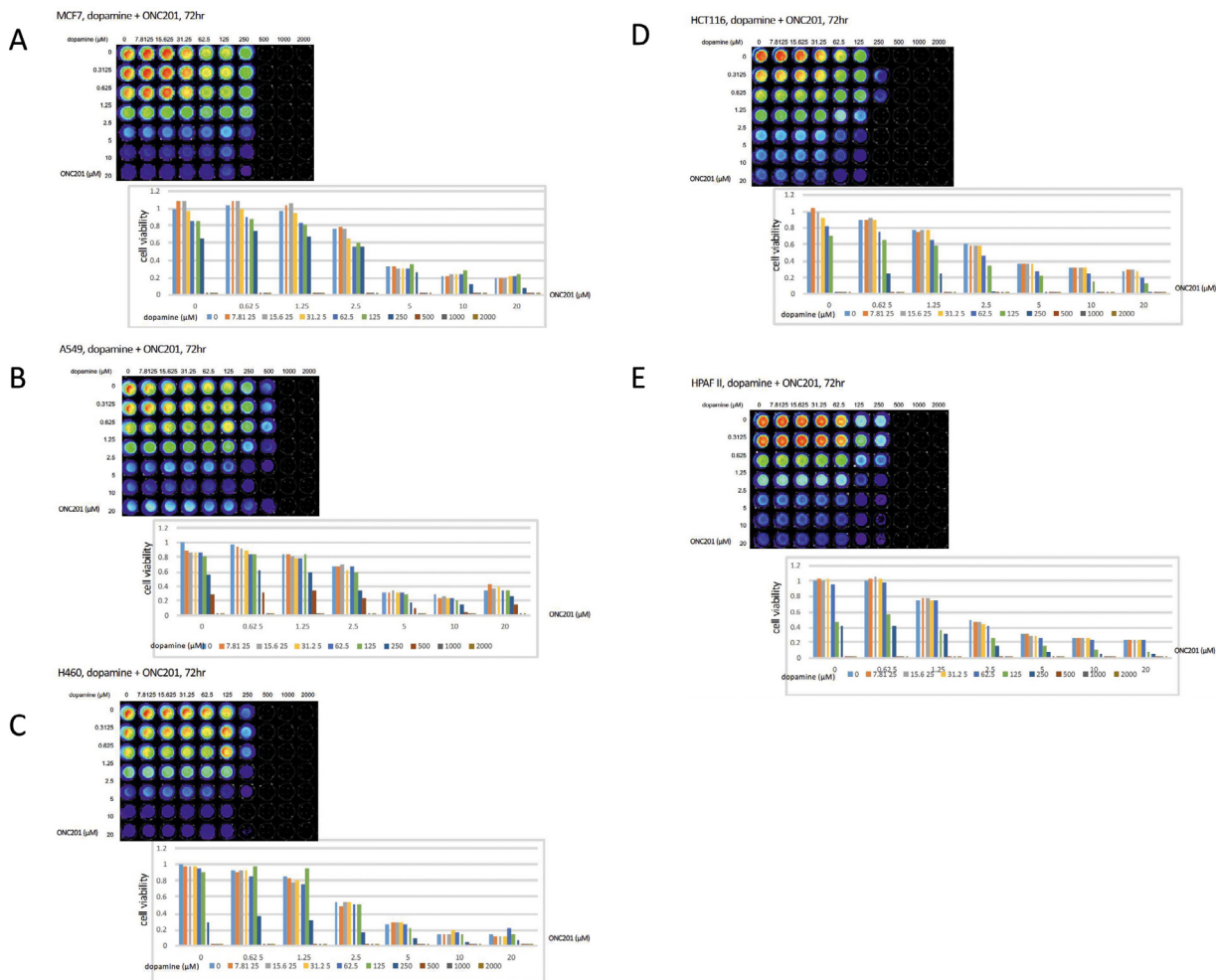


Fig. 12. Effects of dopamine on cell viability of multiple human tumor cell lines treated with ONC201. (A) MCF7 breast, (B) A549 lung, (C) H460 lung, (D) HCT116 colorectal, and (E) HPAF II pancreatic cancer cell lines were treated with drug doses as indicated and CellTiterGlo assays were performed at 72 H.

pancreatic cancer, gastric adenocarcinoma, hepatocellular carcinoma, and multiple myeloma cell lines. The extent of the synergy was different across various tumor cell lines. The synergy was more potent in U251 and HepG2 in which the combination index of ONC201 and EPZ-6438 is less than 0.3 at some dosages (Table S2). We tested another EZH2i, PF-06821497 and revealed that PF-06821497 produced greater synergy when the combined treatment conducted in the same cell lines compared with EPZ-6438 (Table S3, S2), which further supports the combination therapy of EZH2i plus ONC201.

The synergy was evaluated with the CellTiterGlo cell viability assay which detects the amount of ATP directly proportional to the number of cells present in the culture. MDA-MB-468 is sensitive to ONC201 with IC50 of 5.52 μM (Fig. S1A), but a single treatment with ONC201 could not induce PARP cleavage in MDA-MB-468 (Fig. S2B). With the addition of EPZ-6438, synergy was observed in the CTG assay, and PARP cleavage was evident following EPZ-6438 treatment in MDA-MB-468 (Fig. S2C, S2D). ONC201 was originally reported to transcriptionally induce TRAIL and DR5, leading to extrinsic cell death pathway activation and caspase-dependent apoptotic cell death [1, 6, 24]. The fact that ONC201 could not induce PARP cleavage implicates that the suppression of cell viability induced by ONC201 may be due to mechanisms other than caspase-dependent apoptosis, and several growth arrest mechanisms were proposed [24].

It has been demonstrated that EZH2 and HDAC proteins work cooperatively to mediate gene silencing by acting on the same nucleosome(s) [29, 30]. We hypothesize that EZH2i and HDACi may cooperate to open chromatin and induce transcription of target genes. With the addition of vorinostat, the combination of vorinostat, EPZ-6438, and ONC201 demonstrates potent synergies in MCF7, HepG2, Hep3B, MM1S, Saos2, and AGS cell lines (Fig. 4, Table S4) over and above observed synergies with EPZ-6438 and ONC201 (Fig. 1, Fig. S1B, Table S2). However, neither the single treatment with ONC201 at 2.5 μM nor the combination of the three agents could induce caspase 3 or PARP cleavage in AGS cells (Fig. S4C). Thus, the suppression of cell viability in AGS caused by ONC201 or the combination of vorinostat, EPZ-6438, and ONC201 may be due to mechanisms other than caspase-dependent apoptosis.

ONC201 triggers the ISR that is dependent on ATF4 up-regulation and downstream signaling. In the present study, a single treatment with ONC201 induced ATF4 and the addition of EPZ-6438 or vorinostat enhanced the induction of ATF4 in the MCF7, U251, MDA-MB-361, and Saos2 cell lines (Fig. 3, Fig. S3A, S5B). A single treatment of ONC201 also induced ATF4 in the Hep3B cell line, but with the addition of EPZ-6438 or vorinostat, there was no additional enhancement of ATF4 up-regulation (Fig. 6B). Knockdown of ATF4 reduced the cell death after treatment in U251 but increased the cell death in Hep3B. In AGS and

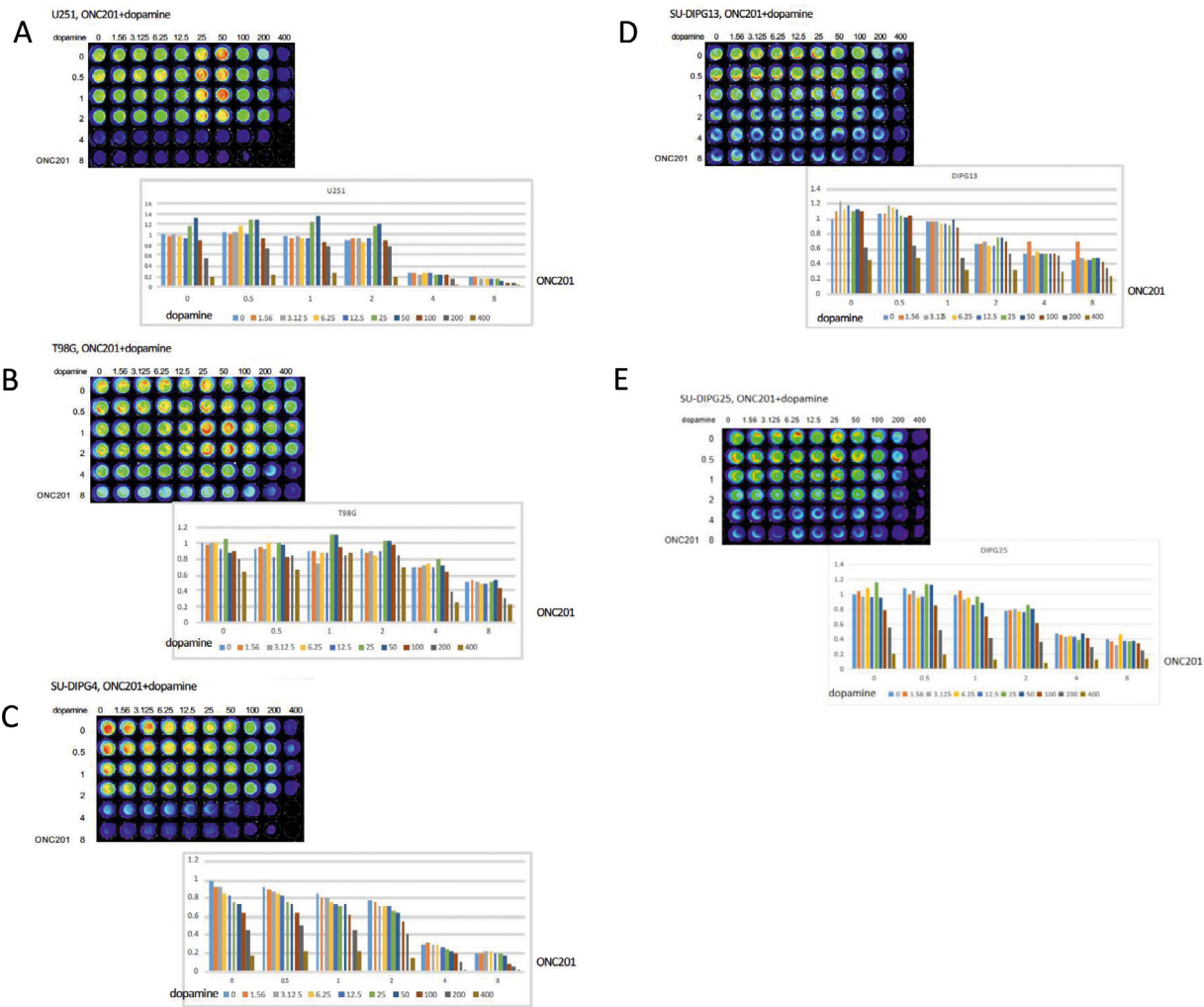


Fig. 13. Effects of dopamine on cell viability of multiple human brain tumor cell lines treated with ONC201. (A) U251 glioma, (B) T98G glioma, (C) DIPG4, (D) DIPG13, and (E) DIPG25 cell lines were treated with drug doses as indicated and CellTiterGlo assays were performed at 72 H. Dopamine and ONC201 concentrations are in μM .

MM1S cell lines, no ATF4 up-regulation was observed with either ONC201 or the combination treatment. Thus, the role of ATF4 in the cell viability suppression or the apoptosis induced by ONC201 or the combination of ONC201 and the epigenetic modulators is different across different tumor types.

ONC201 up-regulates TRAIL, and TRAIL binds to its membrane-bound death receptor DR5 inducing the formation of a death-inducing signaling complex thereby activating the apoptotic cascade. In order to implicate the role of this pathway, we evaluated DR5 expression changes with the different treatments. We observed up-regulation of DR5 in MCF7, U251, and Hep3B by ONC201 and the combinatorial treatment. But we could hardly detect the induction of DR5 in AGS and MM1S cell lines in which the up-regulation of ATF4 was not observed either. Thus, DR5 plays a role in apoptosis caused by ONC201 or the combination of ONC201 and the epigenetic modulators in MCF7, U251, and Hep3B cell lines. However, a mechanism other than the TRAIL pathway may contribute to the tumor cell suppression in AGS and MM1s cell lines.

It has been previously demonstrated that over-expression of the DRD2 receptor increases the extent of apoptosis resulting from ONC201 treatment and that knockdown or pharmacological blockade of DRD5 increases ONC201-induced apoptosis [24]. Moreover, a DRD2+DRD5- biomarker

signature is associated with enhanced ONC201 tumor cell sensitivity [23]. However, in our study, no correlation between mRNA expression of dopamine receptors and ONC201 sensitivity was observed in multiple tumor cell lines ($N = 12$). No correlation was observed as well between altered mRNA expression of dopamine receptors and drug sensitivity after treatment with ONC201 alone or in combination with vorinostat. The lack of detection of endogenous dopamine receptor expression at the protein level is a limitation of this study, although the dopamine receptors were hypothesized to be transcriptionally regulated including through epigenetic modulation. Nevertheless, epigenetic modulation with vorinostat impacts a broad spectrum of targets, so the effects on gene expression are global. Contributing factors towards the sensitization to ONC201 due to vorinostat are therefore complex and remain to be further elucidated. To understand whether DRD2 plays a role in the synergy of the combination of epigenetic modulators and ONC201, we evaluated the impact of the combination of epigenetic modulators and ONC201 on the expression of DRD2 in the tumor cell lines at the protein level. No prominent or stable up-regulation of DRD2 was observed in U251 and AGS cell lines. Up-regulation of DRD2 was observed in MCF7 cells. However, the role of DRD2 in the synergy with ONC201 and the epigenetic modulators still needs to be demonstrated by the knockdown of DRD2.

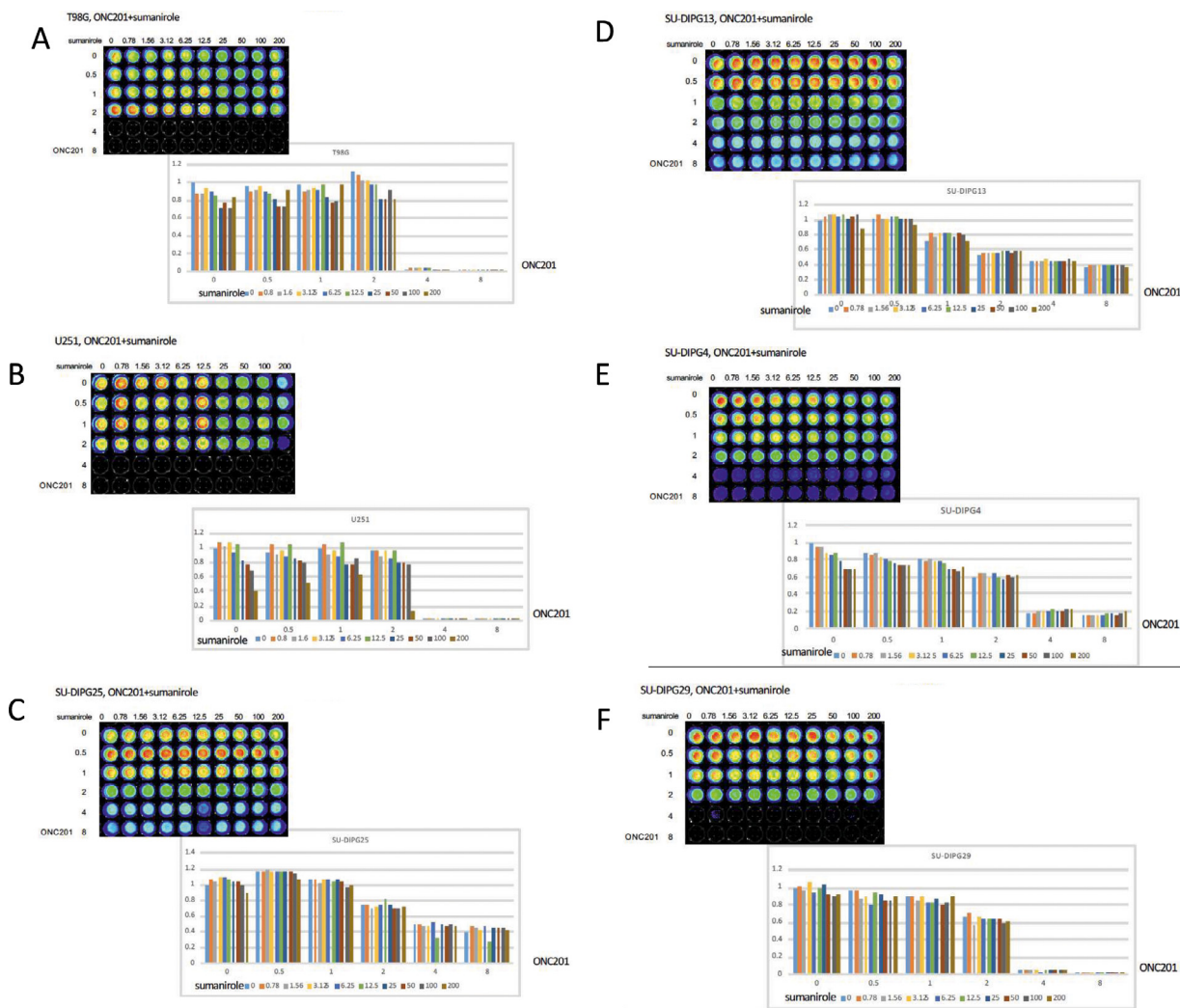


Fig. 14. Effects of DRD2 agonist sumanirole on cell viability of multiple human brain tumor cell lines treated with ONC201. (A) T98G glioma, (B) U251 glioma, (C) DIPG25, (D) DIPG13, (E) DIPG4 and (F) DIPG29 cell lines were treated with drug doses as indicated and CellTiterGlo assays were performed at 72 H. ONC201 and sumanirole concentrations are in μM .

Our results suggest that effects of dopamine or DRD2 agonist sumanirole may be quite limited in overcoming the anti-tumor efficacy of ONC201 at least in multiple cultured tumor cell lines (including DIPG) treated with ONC201. The lack of suppression of ATF4 induction, DR5 induction, or cell death of tumor cells including DIPG cells suggests that those mechanisms may not be overcome by the classical activation of dopamine receptor signaling. The correlation of suppression of cell death by siATF4 argues that the integrated stress response and downstream effects leading to induction of DR5 and apoptosis are relevant for ONC201 mediated apoptosis of multiple tumor cell lines including DIPG cells.

Our studies reveal the synergy of ONC201 plus epigenetic modulators targeting H3K27 *in vitro* and provide a rationale for the combinatorial regimens of ONC201 and epigenetic modulators in tumor therapy. While we hypothesized that reduced methylation as well as increased acetylation of H3K27 might correlate with synergies between epigenetic modulators and ONC201, it was somewhat surprising that only reduced methylation and not necessarily increased acetylation occurred to correlate with cell death with the ONC201 plus epigenetic modulator doublet or triple therapies (ONC201, EPZ-6438, vorinostat). Since these analyses were performed using tumor cells harvested after 72 H incubations with the drugs, it is possible that the

cells with increased acetylation died at earlier time points. This possibility could be further evaluated in the models we used here in future experiments. Moreover, early data in our laboratory in fusion-driven sarcoma models suggest that the cells with the highest acetylation may be eliminated earlier after combinations of ONC201 with HDAC inhibitors (Wen-I Chang and W.S. El-Deiry, unpublished observations). The fact that epigenetic alteration at H3K27 enhances apoptosis due to ONC201 implicates the role of H3K27 in the mechanism of tumor suppression caused by ONC201. Our results suggest that further testing of ONC201 in combination with epigenetic modulators such as EZH2i and HDACi including a triple combination may be pursued further *in vivo* and in the clinic for multiple tumor types.

Author contributions

Yiqun Zhang: Conceptualization; Data curation; Formal analysis; Investigation; Methodology; Validation; Visualization; Roles/Writing – original draft; Writing – review & editing. Lanlan Zhou: Formal analysis; Investigation; Methodology; Writing – review & editing. Howard Safran: Investigation; Writing – review & editing. Robyn Borsuk: Investigation; Writing – review & editing. Rishi Lulla: Investigation; Writing – review

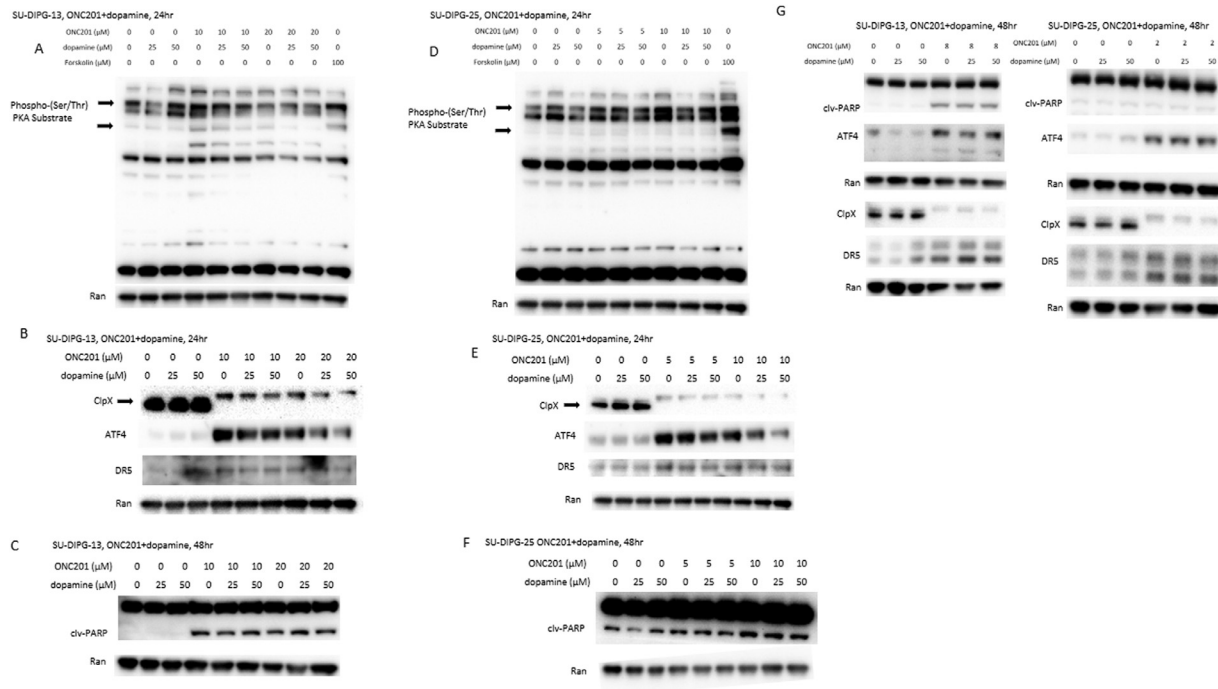


Fig. 15. Dopamine or the DRD2 agonist sumanrirole do not rescue ONC201 mediated loss of cell viability in multiple human tumor cell lines including DIPG. Dopamine effects on ONC201-induced increase in PKA substrate in DIPG13 (A), DIPG25 (D). Effects of dopamine on apoptosis by ONC201 in different tumor cell lines on ATF4 induction, DR5 activation or apoptosis (B,C,E,F,G). In panels A, and D, there are multiple bands that are impacted (increased intensity) by the positive control Forskolin, reflecting phosphorylation of cellular PKA substrates.

& editing. Nikos Tapinos: Investigation; Writing – review & editing. Atila A. Seyhan: Conceptualization; Formal analysis; Writing – review & editing. Wafik S. El-Deiry: Conceptualization; Formal analysis; Funding acquisition; Investigation; Methodology; Project administration; Resources; Supervision; Validation; Visualization; Roles/Writing – original draft; Writing – review & editing.

Acknowledgments

The contents of this manuscript are solely the responsibility of the authors and do not necessarily represent the official views of the National Cancer Institute, the National Institutes of Health, or the American Cancer Society.

Supplementary materials

Supplementary material associated with this article can be found, in the online version, at doi:10.1016/j.neo.2021.06.007.

References

- [1] Kline CL, Van den Heuvel AP, Allen JE, Prabhu VV, Dicker DT, El-Deiry WS. ONC201 kills solid tumor cells by triggering an integrated stress response dependent on ATF4 activation by specific eIF2alpha kinases. *Sci Signal* 2016;9:ra18.
- [2] Ralff MD, Kline CLB, Kucuk OC, Wagner J, Lim B, Dicker DT, Prabhu VV, Oster W, El-Deiry WS. ONC201 demonstrates antitumor effects in both triple-negative and non-triple-negative breast cancers through TRAIL-dependent and TRAIL-independent mechanisms. *Mol Cancer Ther* 2017;16:1290–8.
- [3] Zhang Q, Wang H, Ran L, Zhang Z, Jiang R. The preclinical evaluation of TIC10/ONC201 as an anti-pancreatic cancer agent. *Biochem Biophys Res Commun* 2016;476:260–6.

- [4] Talekar MK, Allen JE, Dicker DT, El-Deiry WS. ONC201 induces cell death in pediatric non-Hodgkin's lymphoma cells. *Cell Cycle* 2015;14:2422–8.
- [5] Prabhu VV, Talekar MK, Lulla AR, Kline CLB, Zhou L, Hall J, Van den Heuvel APJ, Dicker DT, Babar J, Grupp SA, et al. Single agent and synergistic combinatorial efficacy of first-in-class small molecule imipridone ONC201 in hematological malignancies. *Cell Cycle* 2018;17:468–78.
- [6] Allen JE, Krigsfeld G, Mayes PA, Patel L, Dicker DT, Patel AS, Dolloff NG, Messaris E, Scata KA, Wang W, et al. Dual inactivation of AKT and ERK by TIC10 signals Foxo3a nuclear translocation, TRAIL gene induction, and potent antitumor effects. *Sci Transl Med* 2013;5:171ra117.
- [7] Wagner J, Kline CL, Pottorf RS, Nallaganчу BR, Olson GL, Dicker DT, Allen JE, El-Deiry WS. The angular structure of ONC201, a TRAIL pathway-inducing compound, determines its potent anti-cancer activity. *Oncotarget* 2014;5:12728–37.
- [8] Hall MD, Odia Y, Allen JE, Tarapore R, Khatib Z, Niazi TN, Daghistani D, Schalop L, Chi AS, Oster W, et al. First clinical experience with DRD2/3 antagonist ONC201 in H3 K27M-mutant pediatric diffuse intrinsic pontine glioma: a case report. *J Neurosurg Pediatr* 2019;23:1–7.
- [9] Arrillaga-Romany I, Odia Y, Prabhu VV, Tarapore RS, Merdinger K, Stogniew M, Oster W, Allen JE, Mehta M, Batchelor TT, et al. Biological activity of weekly ONC201 in adult recurrent glioblastoma patients. *Neuro Oncol* 2020;22:94–102.
- [10] Chan KM, Fang D, Gan H, Hashizume R, Yu C, Schroeder M, Gupta N, Mueller S, James CD, Jenkins R, et al. The histone H3.3K27M mutation in pediatric glioma reprograms H3K27 methylation and gene expression. *Genes Dev* 2013;27:985–90.
- [11] Margueron R, Reinberg D. The Polycomb complex PRC2 and its mark in life. *Nature* 2011;469:343–9.
- [12] Gan L, Yang Y, Li Q, Feng Y, Liu T, Guo W. Epigenetic regulation of cancer progression by EZH2: from biological insights to therapeutic potential. *Biomark Res* 2018;6:10.
- [13] Yamagishi M, Uchimaru K. Targeting EZH2 in cancer therapy. *Curr Opin Oncol* 2017;29:375–81.

- [14] Mohammad F, Weissmann S, Leblanc B, Pandey DP, Hojfeldt JW, Comet I, Zheng C, Johansen JV, Rapin N, Porse BT, et al. EZH2 is a potential therapeutic target for H3K27M-mutant pediatric gliomas. *Nat Med* 2017;**23**:483–92.
- [15] Wang H, Chen X, Xu Z, Tan Y, Qi X, Zhang L, Xu A, Ren F. Identification of a novel fusion gene, RUNX1-PRPF38A, in acute myeloid leukemia. *Int J Lab Hematol* 2017;**39**:e90–3.
- [16] Yomtoubian S, Lee SB, Verma A, Izzo F, Markowitz G, Choi H, Cerchietti L, Vahdat L, Brown KA, Andreopoulou E, et al. Inhibition of EZH2 catalytic activity selectively targets a metastatic subpopulation in triple-negative breast cancer. *Cell Rep* 2020;**30**:755–70 e756.
- [17] Knutson SK, Kawano S, Minoshima Y, Warholic NM, Huang KC, Xiao Y, Kadowaki T, Uesugi M, Kuznetsov G, Kumar N, et al. Selective inhibition of EZH2 by EPZ-6438 leads to potent antitumor activity in EZH2-mutant non-Hodgkin lymphoma. *Mol Cancer Ther* 2014;**13**:842–54.
- [18] Nakagawa M, Fujita S, Katsumoto T, Yamagata K, Ogawara Y, Hattori A, Kagiyama Y, Honma D, Araki K, Inoue T, et al. Dual inhibition of enhancer of zeste homolog 1/2 overactivates WNT signaling to deplete cancer stem cells in multiple myeloma. *Cancer Sci* 2019;**110**:194–208.
- [19] Eich ML, Athar M, Ferguson JE 3rd, Varambally S. EZH2-targeted therapies in cancer: hype or a reality. *Cancer Res* 2020;**80**:5449–58.
- [20] Li Y, Seto E. HDACs and HDAC inhibitors in cancer development and therapy. *Cold Spring Harb Perspect Med* 2016;**6**.
- [21] Eckschlager T, Plch J, Stiborova M, Hrabeta J. Histone deacetylase inhibitors as anticancer drugs. *Int J Mol Sci* 2017;**18**.
- [22] Madhukar NS, Khade PK, Huang L, Gayvert K, Galletti G, Stogniew M, Allen JE, Giannakakou P, Elemento O. A Bayesian machine learning approach for drug target identification using diverse data types. *Nat Commun* 2019;**10**:5221.
- [23] Prabhu VV, Madhukar NS, Gilvary C, Kline CLB, Oster S, El-Deiry WS, Elemento O, Doherty F, VanEngelenburg A, Durrant J, et al. Dopamine receptor D5 is a modulator of tumor response to dopamine receptor D2 antagonism. *Clin Cancer Res* 2019;**25**:2305–13.
- [24] Kline CLB, Ralff MD, Lulla AR, Wagner JM, Abbosh PH, Dicker DT, Allen JE, El-Deiry WS. Role of dopamine receptors in the anticancer activity of ONC201. *Neoplasia* 2018;**20**:80–91.
- [25] Pakos-Zebrucka K, Koryga I, Mnich K, Ljujic M, Samali A, Gorman AM. The integrated stress response. *EMBO Rep* 2016;**17**:1374–95.
- [26] Zinszner H, Kuroda M, Wang X, Batchvarova N, Lightfoot RT, Remotti H, Stevens JL, Ron D. CHOP is implicated in programmed cell death in response to impaired function of the endoplasmic reticulum. *Genes Dev* 1998;**12**:982–95.
- [27] Zou W, Yue P, Khuri FR, Sun SY. Coupling of endoplasmic reticulum stress to CDDO-Me-induced up-regulation of death receptor 5 via a CHOP-dependent mechanism involving JNK activation. *Cancer Res* 2008;**68**:7484–92.
- [28] Arrillaga-Romany I, Chi AS, Allen JE, Oster W, Wen PY, Batchelor TT. A phase 2 study of the first imipridone ONC201, a selective DRD2 antagonist for oncology, administered every three weeks in recurrent glioblastoma. *Oncotarget* 2017;**8**:79298–304.
- [29] Varambally S, Dhanasekaran SM, Zhou M, Barrette TR, Kumar-Sinha C, Sanda MG, Ghosh D, Pienta KJ, Sewalt RG, Otte AP, et al. The polycomb group protein EZH2 is involved in progression of prostate cancer. *Nature* 2002;**419**:624–9.
- [30] Zhang T, Cooper S, Brockdorff N. The interplay of histone modifications - writers that read. *EMBO Rep* 2015;**16**:1467–81.